In-situ zircon U-Pb, oxygen and hafnium isotopic evidence for magma mixing and mantle metasomatism in the Tuscan Magmatic Province, Italy

Gagnevin D.[1]

Daly J.S.[1]

Horstwood M.S.A.[2]

Whitehouse M.J.[3]

[1]UCD School of Geological Sciences, University College Dublin, Belfield, Dublin 4, Ireland

[2]NERC Isotope Geosciences Laboratory, British Geological Survey, Keyworth, Nottingham, UK

[3]Laboratory for Isotope Geology, Swedish Museum of Natural History, Stockholm, Sweden

Submit revisions before Feb 17, 2011

Submitted to: *Earth and Planetary Science Letters*

1 Table, 6 Figures, 6 Electronic Supplementary Materials

* Corresponding author: Damien.Gagnevin@ucd.ie; tel (+353) 1716 2326; Fax (+353) 1283 7733

Abstract

In this study, we have used *in-situ* U-Pb, Hf and O isotopic analyses in zircon grains to gain insights into both magmatic processes and duration of magmatism in igneous rocks from the Tuscan Magmatic Province (0.1-9 Ma), Italy. Three plutonic centres have been investigated (Monte Capanne and Porto-Azzuro monzogranites in Elba and the Giglio monzogranite) as well as Capraia, the only volcanic centre in the Tuscan Archipelago. New ion microprobe zircon U-Pb data reveal a continuum of plutonic activity in Elba over 2-Ma (8.3-6.3 Ma), with coeval volcanic activity in Capraia (7.1-7.6 Ma), and plutonic activity resuming in Giglio (5.5 Ma) after a gap of 1 Ma. From these zircon data we also show that construction of the Monte Capanne pluton (Elba) may have occurred over a period of c. 0.5 Ma. A significant range of both ^{176}Hf/^{177}Hf (determined by LA-MC-ICPMS) and δ^{18}O (determined by ion microprobe) in zircon (~7 epsilon Hf units and ~5‰, respectively) is present, which, together with zircon morphology and trace element data (Gagnevin et al., 2010), emphasise the importance of mixing and replenishment involving magma batches with both metaluminous and peraluminous affinities. Inherited and xenocrystic zircons also occur, but are scarce. These have a wide range of ^{176}Hf/^{177}Hf and δ^{18}O composition, further emphasising that a variety of crustal components have contributed to the genesis of the Tuscan magmas, either as contaminants or magma sources. While mixing undoubtedly occurred between mafic (metaluminous) and felsic (peraluminous) magmas, the range of Hf and O isotopic data suggest a diversity within the peraluminous component. The unradiogenic Hf composition (εHf*(t)*<-4) and relatively heavy δ^{18}O signature (>6‰) of the inferred mantle-derived component (represented by Capraia volcanism, and at least in part, lamproitic in composition) strongly supports the idea that the mantle source involved in Tuscan magmatism was severely modified by subduction-related, crustal-derived metasomatic fluids.

1. Introduction

The geochemistry of zircon is now widely used to investigate the petrogenesis of igneous rocks (Harley and Kelly, 2007, and references therein), and, in some cases, may help to address the genetic relationship between coeval eruptive and intrusive rocks (e.g., Kemp et al., 2006). The crystallization or resorption history of zircon has been shown to be texturally and chemically responsive to interaction between chemically-contrasting melt components (Griffin et al., 2000; 2002; Flowerdew et al. 2006; Yang et al., 2006; 2007; Kemp et al., 2005; 2006; 2007; Hawkesworth and Kemp, 2006; Chu et al., 2006; Reid et al., 2007; Belousova et al., 2006; Appleby et al., 2008; Bolhar et al., 2008; Shaw and Flood, 2009). Magma mixing is thought to have a major role in governing the petrogenesis of intermediate to acidic rocks in the long-lived (9-0.2 Ma) Tuscan Magmatic Province (TMP, Tuscany, Italy) (Poli, 1992, 2004; Innocenti et al., 1992; Serri et al., 1993; Westerman et al., 1993; Dini et al., 2002; 2004; 2008; Gagnevin et al., 2004; 2005a, b; 2008a, 2010). The earlier evolution of the TMP (from 9 to 5 Ma) is exemplified by excellently exposed plutonic and volcanic rocks in the Tuscan Archipelago. Magmatism in the Elba plutonic complex and the Capraia volcano has been suggested to be coeval (e.g., Ferrara and Tonarini, 1985; Aldighieri et al. 1998).

An earlier study (Gagnevin et al., 2010) on the chemistry and morphology of zircon in the Monte Capanne plutonic complex and Capraia has been extended using *in-situ* hafnium (Hf) and oxygen (O) isotopic analyses ($^{176}Hf/^{177}Hf$ and $\delta^{18}O$, respectively), coupled with *in-situ* U-Pb geochronology. In this study samples have been analysed from Elba, Capraia and Giglio (Fig. 1). The aim was to try to better define the age of magmatism, to evaluate how zircon in a young plutonic setting can record a magma mixing signal and better constrain the nature of the end members involved in mixing
In-situ U-Pb zircon dating has been carried out to distinguish magmatic from inherited zircon grains and in some cases to improve upon the existing geochronology.

The petrogenesis of the Capraia volcano, located at the northern end of the archipelago (**Fig**. 1), is of particular interest as it is the only volcanic edifice in the archipelago, and provides clear evidence of mixing between mantle-derived, high K calc-alkaline and lamproitic magmas, associated with crystal fractionation, as indicated by major element modelling (Poli and Perugini, 2003) and plagioclase zoning patterns (Gagnevin et al., 2007). Lamproitic magmatism is also common in the Tuscan mainland, and has been attributed to mantle metasomatism associated with subduction based on a variety of petrological data, including Sr, Nd and Pb isotopic ratios (e.g., Conticelli et al., 2009). It is, however, of particular interest whether zircon, in both Capraia and the Tuscan plutonic rocks has recorded this peculiar geochemical signature.

A detailed zircon Hf and O isotopic investigation, coupled with U-Pb geochronology, on individual magmatic centres in the Tuscan archipelago, with particular emphasis on the Monte Capanne pluton and coeval Capraia volcanism, is likely to 1) further reveal the nature of the magma components involved in magma mixing, 2) decipher the open-system history of individual magma centres (with emphasis on the Monte Capanne pluton, Elba), and 3) provide some insights into the long-debated relationships between intrusive and extrusive magmatism (Kemp et al., 2006; Bachmann et al., 2007, and references therein). These data will therefore further reappraise models for the petrogenesis of the Tuscan magmatism.

2. Geological background: the Tuscan Magmatic Province (TMP).

Calc-alkaline to potassic magmatism in the TMP (**Fig**. 1a) is classically considered to be contemporaneous with the opening of the Tyrrhenian Sea (in the late Miocene) following the collision and subduction of the Adriatic below the Corsica-Sardinia microplate (Principi and Treves, 1984; Serri et al., 1993). Magmatic activity in the TMP, which progressively migrated from west to east as a result of slab roll-back and retreat of the Adriatic slab (e.g. Serri et al., 1993; Brunet et al., 2000), spans a range of c. 8 Ma. Plutonic and volcanic rocks occur in about equal proportions, though plutonic rocks predominate in the Tuscan Archipelago, while volcanic rocks occur mainly on the Italian mainland. The Tuscan Archipelago comprises the Elba, Giglio and Montecristo plutonic systems (Fig. 1). These have typical S-type signatures implying an origin by large-scale anatexis of supracrustal rocks (Taylor and Turi, 1976; Giraud et al., 1986), though the involvement of a mantle-derived component through magma mixing with anatectic magmas is well established based on whole rock geochemical (e.g., Poli, 1992) and isotopic studies (Dini et al. 2002, Gagnevin et al., 2004). The 7-8 Ma-old Capraia volcanic centre (north of Elba; **Fig**. 1a) comprises high-K calc-alkaline to shoshonitic lavas/domes inferred to have a mantle origin (Poli and Perugini, 2003; Chelazzi et al., 2006; Gagnevin et al., 2007).

3. Analytical methods

Samples were split into 2-4 cm cubes, washed, dried and crushed in a tungsten carbide jaw crusher. Zircon was separated from <250 µm sieved fractions using standard heavy liquid techniques, hand-picked and mounted in epoxy resin. All studied grains were imaged by scanning electron microscopy using back-scattered (BSE) and cathodoluminescence detectors. A subset of grains was also analysed by electron microprobe (Gagnevin et al. 2010).

U-Th-Pb zircon analyses were performed by secondary ion mass spectrometry (SIMS) on the Cameca IMS 1270 ion-microprobe at the Swedish Museum of Natural History (NORDSIM Laboratory) as described by Whitehouse and Kamber (2005) using a spot size of c. 25 um. U/Pb ratio calibration was based on analyses of the reference zircon 91500, which has an age of 1062 Ma and U and Pb concentration of 80 ppm and 15 ppm, respectively (Wiedenbeck et al., 1995). Age calculations were made using Isoplot version 3.2 (Ludwig, 2003). Following Zeck and Whitehouse (2002), common lead corrections were applied using a modern-day average terrestrial common lead composition, i.e., $^{207}Pb/^{206}Pb = 0.83$ (Stacey and Kramers, 1975), where significant ^{204}Pb counts were recorded.

Lu-Hf isotopic analyses were carried out at the NERC Isotope Geosciences Laboratory (NIGL) in Nottingham, using a Nu Instruments Nu-Plasma HR multi-collector ICP-MS coupled to a New Wave Research UP193SS 193nm solid state laser ablation system. The full protocol for laser ablation MC-ICPMS Hf analyses can be found in the Electronic Supplementary Material A.

Oxygen isotopic analyses were carried out on the Cameca IMS 1270 ion-microprobe following methods described by Whitehouse and Nemchin (2009). The mount stage xy and DT1 centering diagrams for all O analyses can be found in Electronic Supplement Material B. The DT1 values (when corrected for a 1270 vs. 1280 scaling factor of ca.0.5) fall within the range of values found by Whitehouse and Nemchin (2009) to yield acceptable results over a wide area of the mount. Measured isotopic ratios were normalised to a $\delta^{18}O$ value of +9.86‰ (SMOW) for the reference zircon 91500 (Wiedenbeck et al., 2004).

4. Samples

Ten samples were investigated in this study (**Fig**. 1b), including seven samples from the Monte Capanne (MC) plutonic system, one from the granite porphyry (DG259), one from the Porto-Azzurro granite (DG23), one from the Giglio monzogranite (DG264) and one dacite from Capraia (DG05-1). Samples from the Monte Capanne plutonic system include three monzogranites (representing the bulk of the MC pluton; DG236, DG314 and DG316), two mafic microgranular enclaves (hosted in the MC monzogranites; DG210 and DG220), and one mafic Orano dyke (cutting the MC monzogranite; DG135). Most of these samples are well characterised petrographically, chemically (major and trace elements) and isotopically (Sr and Nd) (Gagnevin et al., 2004). In particular, they display a range of chemical (Zr = 115-180 ppm; K_2O = 2.2-4.8 wt%) and isotopic ($Sr_{(i)}$ = 0.714-0.717; $Nd_{(i)}$ = 0.51210-0.51222) compositions. For other samples where whole-rock data are presently not available (DG236, DG05-01, DG23 and DG264), we refer to other studies to constrain their bulk composition. Briefly, samples DG236 and DG05-01 are inferred on the basis of the petrography to be chemically and isotopically similar to other monzogranitic samples from the Sant' Andrea facies in the Monte Capanne pluton (SiO_2 > 60%, Zr ~ 150 ppm, $Sr_{(i)}$ = 0.714-0.717) and other dacites in Capraia (SiO_2 > 58%, Zr ~ 200 ppm, $Sr_{(i)}$ = 0.710), respectively (Dini et al., 2002; Gagnevin et al. 2007;

2008a). Following other studies (Poli et al., 1989; Poli, 1992; Westerman et al., 1993), the Zr content of the Giglio sample (DG264) is anticipated to be around 100-200 ppm, with rather homogenous $Sr_{(i)}$ (0.717-0.718). Similarly, the Porto Azzurro monzogranite (sample DG23) has a very limited range of chemical (Zr = 108-157 ppm) and isotopic ($Sr_{(i)}$ = 0.713) compositions (Conticelli et al., 2001).

5. Zircon size, texture and chemistry

Extensive U-Pb analysis by both ion microprobe and laser-ablation ICPMS methods have enabled us to distinguish confidently between "magmatic" and "xenocrystic" zircons. The morphology, internal textures and chemical compositions of zircons considered to be "magmatic" from both the MC plutonic system and Capraia are described elsewhere (Gagnevin et al., 2010). All back-scattered images for the MC plutonic system and Capraia are presented in Electronic Supplementary Material C, which also indicates the position of the O, Hf and U-Pb analytical spots.

Briefly, grain size varies between 90µm - 260µm in the MC plutonic system. Patchy-zoning, which results from replacement of original U-Th-Y-rich zircon by U-Th-Y-poor zircon, is the most common textural type in the zircon cores, and is almost systematically accompanied by pores of various size (**Fig**. 2a, b). Patchy-zoning is followed by compositionally variable (alternating U-Th-Y-poor and U-Th-Y-rich domains) oscillatory zoning (**Fig**. 2a, b). Although less common, homogeneous, U-Th-Y-poor, zircon cores (**Fig**. 2c) also occur in most magma products, including one mafic enclave (DG220).

Zircons in the granite porphyry (DG259; **Fig**. 2d) and the Capraia dacite (DG05-1; **Fig**. 2f) tend to be larger (150-300µm and 180-450µm, respectively) than those from the MC pluton (90-260µm). Zircons in the granite porphyry mainly consist of homogenous, euhedral to subhedral cores followed by compositionally variable oscillatory zoning, occasionally punctuated by resorption surfaces (**Fig**. 2d). Oscillatory zoning is the main textural type in the Capraia dacite (DG05-1; **Fig**. 2f), but unlike zircons in the porphyry or the MC pluton, sharp intra-grain U-Th gradients (bright in BSE) are rarely observed.

Zircons in the Porto Azzurro sample (DG23) have very similar habit, size and texture to those in the MC pluton. Zircon grains in the Giglio sample (DG264) are dominated by homogenous, low U-Th cores with oscillatory-zoned rims.

Inherited cores and xenocrystic zircons occur in all plutonic rocks, but are absent in the Capraia dacite. Xenocrystic zircons are anhedral to subhedral, lack magmatic overgrowths and are depleted in most trace/minor elements (Gagnevin et al., 2010). They are especially abundant in monzogranite DG316. Overall, inherited cores with oscillatory-zoned magmatic overgrowth; **Fig**. 2e) are exceedingly rare, but occur in almost all magma products.

6. Results

6.1. U-Pb data

Forty-four ion microprobe analyses from thirty zircon grains of magmatic origin from seven samples are presented in Table 1. These include six grains from the Monte Capanne plutonic system, five grains from the granite porphyry, thirteen grains from the Capraia dacite, three from the Porto Azzurro pluton and three from the Giglio monzogranite. A larger U-Pb zircon data set is presented in Electronic Supplementary Material D. Of these, acceptable ages were obtained only from zircons with U contents less than 3000 ppm (**Table** 1). Ages from zircons with higher U contents are considered unreliable because a strong correlation was observed (see diagrams in Electronic Supplementary Material D) between the apparent age and the U concentration above 3000ppm (up to 3 wt%). This may be due to U-dependent changes in sputtering and secondary ionisation efficiency (cf. Butera et al.; 2001). U-Pb Concordia diagrams are reported in **Fig**. 3a for the plutonic rocks and in **Fig**. 3b for the Capraia volcanic sample (DG05-1). U-Pb ages were calculated using the Isoplot/Ex 3.0 program of Ludwig (2003). Individual spot ages are reported at 2σ level (Table 1).

$^{206}Pb/^{238}U$ ages for the MC plutonic system (i.e., monzogranite, MME and Orano dyke; **Table** 1) range from 7.62 ± 0.24 Ma (grain 21, DG135) to 7.00 ± 0.38 Ma (grain 21, DG236) (**Fig**. 3c; **Table** 1). Six data points (from 4 grains) give a weighted mean

$^{206}Pb/^{238}U$ age of 7.19 **±** 0.08 Ma (**Fig**. 4a), which is within the range of biotite K-Ar ages (7.1-7.6 Ma; Ferrara and Tonarini, 1985). The two grains (DG135-21 and DG236-4) that are older (7.5-7.6 Ma, **Table** 1) are tentatively interpreted as being antecrystic (see Miller et al. 2007). Juteau et al. (1984) have reported even younger TIMS U-Pb ages (6.2 ± 0.2 Ma) for the main monzogranite, but the data are discordant and will not be considered any further.

Zircons in granite porphyry sample DG259 yield $^{206}Pb/^{238}U$ ages from 8.34 ± 0.40 Ma to 7.84 ± 0.26 Ma (**Table** 1), in line with Rb-Sr and K-Ar ages (range of 7.5 to 8.5 Ma; Ferrara and Tonarini, 1985; Dini et al., 2002). Nine data points (from 5 grains) define a weighted mean $^{206}Pb/^{238}U$ age of 8.08 ± 0.09 Ma (**Fig**. 4c), suggesting that the porphyry body precedes the main phase of crystallization of the MC plutonic system by at least 0.4 Ma.

Zircons in the Capraia dacite (sample DG05-1) yield a range of $^{206}Pb/^{238}U$ ages from 7.0 to 7.6 Ma (**Table** 1), in agreement with K-Ar ages (Aldighieri et al., 1998; Ferrara and Tonarini, 1985), though older K-Ar ages (up to 9.5 Ma) have also been reported from Capraia (Ferrara and Tonarini, 1985). 13 data points (from 9 grains) define a weighted mean $^{206}Pb/^{238}U$ age of 7.29 ± 0.05 Ma (**Fig**. 4b), which is within error of the age of the MC plutonic system. Grain 3 and the rim of grain 6 define the youngest (6.98 ± 0.18 Ma) and oldest (7.60 ± 0.18 Ma) ages, respectively (**Table** 1).

Three zircon ages from the Porto Azzurro monzogranite (sample DG23) range from 6.39 ± 0.22 Ma to 6.67 ± 0.26 Ma (**Table** 1). Three analyses (from 3 grains) define a weighted mean of 6.53 ± 0.39 Ma (**Fig**. 4d), which is also slightly older than K-Ar ages previously reported (5.9-6.2 Ma; Ferrara and Tonarini, 1985; Saupé et al., 1982).

Zircons in the Giglio monzogranite (sample DG264) also display a range of $^{206}Pb/^{238}U$ ages (from c. 5.1 Ma to 5.6 Ma; **Table** 1). The youngest age (5.14 ± 0.34 Ma) was obtained from the core of grain 3 (analysis n2198-3b; **Table** 1) and may reflect some lead loss because another analysis from the same region of this grain (analysis n2198-3c; **Table** 1) is slightly older within error (5.54 ± 0.42 Ma). Excluding the younger age, a weighted mean $^{206}Pb/^{238}U$ age of 5.52 ± 0.14 Ma is obtained (**Fig**. 4e), which is marginally older than the K-Ar ages (5.0 ± 0.2 Ma) obtained by Ferrara and Tonarini (1985).

6.2. Hf isotopic data

A total of seventy-five zircon grains of magmatic origin have been analysed for Lu-Hf isotopes by *in-situ*, laser ablation MC-ICPMS. In the text, individual data points (e.g., DG264-7) are cited by combining the sample number (DG264) with the grain number (7) as listed in Electronic Supplementary Material E. The data are summarised graphically in **Fig.** 5a**.** Lu-Hf data are also reported in relation to the zircon texture (from BSE images) in grains where both types of data are available (i.e., mainly the MC pluton and Capraia dacite; Electronic Supplementary Material C). When grains were sufficiently large, both core and rim were analysed. In twenty instances, Hf was analysed on the same spot (or close to) where U-Pb data were obtained. This, however, was not systematically the case, particularly as the small size of some grains prevented both isotopic measurements on the same growth zone. In other cases, despite co-located U-Pb and Lu-Hf analyses, the high uranium content, as frequently encountered in our dataset, prevented accurate age determinations, and the U-Pb data had to be discarded. No radiogenic growth correction was necessary to determine the initial $^{176}Hf/^{177}Hf$, εHf*(t)* and T_{DM} because of their young ages and low Lu/Hf ratios. Thus, measured and initial ratios are considered to be identical (e.g., Reid et al., 2007).

The most important results arising from these data are summarized below:

1) Zircons of magmatic origin in the Tuscan plutonic rocks record a range of $^{176}Hf/^{177}Hf$ (0.28245-0.28267, corresponding to ~7 epsilon Hf units; **Fig.** 5a) and depleted mantle model ages (T_{DM} from 800 Ma to 1100 Ma; Electronic Supplementary Material E). This range excludes the rim of zircon DG264-7 (Giglio), which exhibits the least radiogenic Hf of all zircons ($^{176}Hf/^{177}Hf$ = 0.28219), rimming a core whose Hf signature is within the above-mentioned range ($^{176}Hf/^{177}Hf$ = 0.28253). Outside of analytical uncertainty, only a few samples (such as DG236 and DG314; **Fig.** 5a) definitely record a range in $^{176}Hf/^{177}Hf$.

2) Zircons in the Capraia dacite (DG05-1) have a homogenous Hf isotopic composition (mean $^{176}Hf/^{177}Hf$ = 0.28260 ± 0.00001; MSWD = 0.77; n = 12), with average εHf*(t)* ~ -6 and T_{DM} ~ 875 Ma (Electronic Supplementary Material E). Within

uncertainty, this volcanic rock overlaps the most radiogenic component in the plutonic samples (mean $^{176}Hf/^{177}Hf = 0.28263 \pm 0.00002$; MSWD = 2.7; n = 10; **Fig.** 5a).

3) Except in very few cases (see below), differences in Hf isotopic composition between zircon cores and rims could not be resolved outside of analytical uncertainty.

4) In general, there is no obvious correlation between the zircon textures, or extent of resorption, and the Hf isotopic composition.

5) Overall, there are no clear changes in $^{176}Hf/^{177}Hf$ with time (**Fig.** 6), i.e., the granite porphyry sample DG259 (oldest) has $^{176}Hf/^{177}Hf$ values similar to those of the Porto Azzurro sample DG23 and Giglio sample DG264 (youngest).

6.3. Oxygen isotopic data

Forty-four zircon grains of magmatic origin have been analysed for oxygen isotopes by SIMS. **Fig.** 5b and Electronic Supplementary Material F report all available oxygen isotopic analyses, adopting the same nomenclature as for Hf. When possible, both cores and rims were analysed. Because the oxygen data were acquired after the Hf laser ablation analyses, the laser pits and the ion microprobe spots do not coincide exactly. However, as far as possible, we have targeted the oxygen analyses to be close to the Hf laser pits within the same compositional or petrographic zone (cf. Gagnevin et al., 2010). Care was taken to avoid previous U-Pb analytical spots to avoid the possible effects of the oxygen primary beam used in SIMS dating. We report the $\delta^{18}O$ values measured in zircon ($\delta^{18}O_{Zc}$) as opposed to $\delta^{18}O$ inferred to represent the value of the melt ($\delta^{18}O_{melt}$) (**Fig**. 5b; see below).

The most important results arising from these data are summarized below:

1) Zircons in both plutonic and volcanic samples record a range of $\delta^{18}O_{Zc}$ (7.1-11.4‰ and 5.9-7.5‰, respectively) (**Fig.** 5b). Thus, except in one case (grain DG264-1; $\delta^{18}O$ = 7.1‰), plutonic and volcanic zircons have a distinct O isotopic signature, although the $\delta^{18}O_{Zc}$ difference between the two is generally < 1‰ (**Fig.** 5b). The highest $\delta^{18}O_{Zc}$ was recorded in the oscillatory-zoned rim of grain DG23-38 (P. Azzurro) (19.2‰; not plotted

in Figs. 8-9 because it is out of scale), which has an inherited core (Electronic Supplementary Material F).

2) Zircons in the Capraia sample DG05-1 record heavier values (up to 7.5‰) than zircons in typical mantle-derived magmatic rocks (5.7 ± 0.5‰; Eiler et al., 1998) or peridotitic mantle rocks (5.3 ± 0.3‰; Valley et al., 1998) (**Fig.** 5b).

3) Intra-grain zircon $\delta^{18}O$ isotopic heterogeneities also in both plutonic and volcanic samples. In the MC plutonic system, $\delta^{18}O_{Zc}$ varies from 8.6‰ in the core of grain DG314-55 (monzogranite) to 10.0‰ in the rim, and from 8.2‰ in the core of DG259-23 (granite porphyry) to 10.0‰ in the rim (Electronic Supplementary Material F). Otherwise, no clear difference in $\delta^{18}O_{Zc}$ is observed between cores (average 9.31 ± 0.47‰) and rims (average 9.87 ± 0.29‰), though we note a slight tendency for the rims to have heavier oxygen values. In the Capraia dacite (DG05-1), intra-grain zircon $\delta^{18}O_{Zc}$ variations are also present, i.e., grains 1 and 10 have rims heavier than cores (e.g. **Fig**. 2f), though most of other grains do not display any significant changes in $\delta^{18}O_{Zc}$.

(4) As for Hf isotopes, there is no clear change in $\delta^{18}O_{Zc}$ with time.

7. Discussion

7.1. Reappraisal of geochronology and implications

Overall, our new *in-situ* zircon U-Pb data are in broad agreement with published Ar-Ar, K-Ar and Rb-Sr ages (Ferarra and Tonarini, 1985; Dini et al., 2002), with slightly younger ages obtained for the Giglio and Porto Azzurro intrusions. An age of 7.2 Ma is likely to represent the main zircon crystallisation phase in the MC pluton, though the rather large uncertainty as well as the occurrence of older, antecrystic zircons grain (7.5-7.6 Ma) indicate that zircon crystallisation in the MC plutonic system may have occurred over at least 0.5 Ma. We note that antecrystic zircons in the Capraia dacite have similar ages to those in the MC plutonic system (7.5-7.6 Ma),

From the new U-Pb data (**Fig.** 3), it appears that igneous activity in Elba occurred almost continuously over a period of about 2 Ma - from the porphyry (DG259; ~8.3 Ma) to the Porto Azzurro monzogranite (DG23; ~6.3 Ma). This c. 2 Ma duration of magmatism is similar to the incremental assembly of plutonic bodies by successive magma pulses inferred from zircon geochronology (Coleman et al., 2004; Glazner et al., 2004; Matzel et al., 2006). Assembly of the MC plutonic system may have been even shorter (0.5-1.0 Ma), as also suggested by Pb diffusion modelling in K-feldspar (Gagnevin et al., 2005b). Our data suggest that the main phase of volcanic activity in Capraia (7.3 Ma) was coeval (within error) with the MC plutonic system (7.2 Ma), providing clear evidence for a close relationship between plutonic and volcanic igneous activity within the early stage of evolution of the Tuscan Magmatic Province.

We note from these U-Pb data that intrusion of the Giglio pluton (DG264; ~5.5 Ma) occurred a million years after that of the Porto Azzurro pluton (DG23; ~6.5 Ma). This gap may be correlated with compressive phases of deformation affecting the inner domain of the Apennine orogenic belt at that time (Boccaletti et al., 1997).

7.2. Zircon as magma mixing tracer in plutonic rocks

Intra-grain Hf and/or O isotopic heterogeneities in zircon are common in granitic rocks (e.g., Kemp et al., 2006; 2007). In this study, zircon records a range of Hf (**Fig**. 5a) and O (**Fig.** 5b) isotopic compositions outside analytical uncertainty. Moreover, $^{176}Hf/^{177}Hf$ and $\delta^{18}O$ are negatively correlated in the plutonic rocks, i.e., high $^{176}Hf/^{177}Hf$ corresponds to low $\delta^{18}O$ (**Fig.** 5a, b). Such a correlation precludes that high $\delta^{18}O$ in Tuscan magmas is caused exclusively by meteoric-hydrothermal alteration (Taylor and Turi, 1976), as Hf in zircon is hardly remobilised during secondary processes such as weathering or hydrothermal alteration (Hawkesworth and Kemp, 2006). Rather, these zircon geochemical features can be explained by two magmatic processes, crustal contamination and/or magma mixing, as discussed below.

In granitic rocks, crustal contamination may be the cause of Hf and O isotopic disequilibria in zircon (e.g., Kemp et al., 2006; 2007; Yang et al., 2007). The occurrence of xenocrystic zircons and inherited cores in both Elba and Giglio (Daly et al., 2007; Gagnevin et al., 2010), together with metasedimentary xenoliths displaying petrographic evidence of melt-forming reactions (Gagnevin, 2005), suggest that interactions with contaminated melts are likely to have occurred. Contamination may provide a plausible explanation to account for the correlation between high $\delta^{18}O$ and unradiogenic Hf (**Fig.** 8). However, it is unlikely to explain the general pattern because 1) inherited cores (with magmatic overgrowth) are rare in the Tuscan plutonic rocks (**Table** 1; Daly et al., 2007; Gagnevin et al., 2008b) and 2) xenocrystic zircons (lacking magmatic overgrowth) are not widespread and only occur in specific samples having Sr and Nd isotopic values suggestive of crustal contamination (e.g. sample DG316, Gagnevin et al., 2004). This suggests that contamination with crust was only localised into melt pockets shortly before emplacement, rather than being a feature of the entire magmatic history.

Instead, the magma mixing hypothesis is preferred to explain the textural and geochemical features of zircon in the plutonic rocks (e.g., Griffin et al., 2002; Shaw and Flood, 2009). Zircons in the MC pluton, which is the most extensively studied intrusion in the Tuscan Archipelago, have textures (such as patchy-zoned cores; **Fig.** 2a, b) and an exceptionally wide range of trace/minor element content identified by electron microprobe analyses (Gagnevin et al., 2010) that are suggestive of magma mixing (Gagnevin et al., 2010). Generally, the range of Hf and O in zircon is unrelated to textural changes (**Fig.** 2). However, we note that zircon grains in mafic enclave DG210, which display cores with patchy-zoning (Electronic Supplementary Material C), have unradiogenic Hf (down to $^{176}Hf/^{177}Hf = 0.28245$) and elevated $\delta^{18}O_{Zc}$ (> 9.8‰). Despite its occurrence in a mafic enclave, this zircon isotopic signature, together with high trace element abundances (U>10,000-20,000 ppm; Gagnevin et al., 2010), is interpreted as reflecting initial crystallisation in a silicic melt. It is thus possible that zircons in such enclaves may reflect initial mechanical transfer of zircon from high-U-Th silicic magmas into low-U-Th mafic magmas after magma replenishment, which in turn caused resorption. Subsequent quenching permanently preserved these zircons within the enclave.

In other cases, intra-grain core-to-rim variations towards unradiogenic Hf (e.g., DG314-55, Electronic Supplementary Material E) and elevated $\delta^{18}O_{Zc}$ (e.g., DG314-55 and DG259-23; Electronic Supplementary Material F) support zircon transfer between radiogenic Hf, low $\delta^{18}O$, melts and unradiogenic Hf, high $\delta^{18}O$ melts during/after recharge. In the case of DG259-23, which has been imaged by SEM (**Fig**. 2b), increase in $\delta^{18}O_{Zc}$ from core to rim is coupled with resorption, suggesting periods of zircon undersaturation and regrowth during transfer between different melt batches.

The similarity in $\delta^{18}O_{Zc}$ and $^{176}Hf/^{177}Hf$ between core and rim, as frequently encountered in our dataset, may provide evidence for partial dissolution of initial high-U-Th zircon followed by closed-system regrowth in similar melt batches, possibly in the source region (Flowerdew et al., 2006). In this particular case, one would expect rims to have a Hf isotopic composition similar to that of the surviving inherited zircon cores, which is not observed here, as rims seem to preserve distinct Hf signature compared to the inherited cores (e.g. grain 12, DG220; grain 23, DG23; grain 7, DG264; Electronic Supplementary Material E). In the hypothesis where high U-Th zircon occurs at a higher crustal level, patchy-zoning in the zircon cores might be accounted for by resorption following repeated input of hot silicic melts derived from the same magma source (hence having similar Hf isotopic signature). Therefore, mixing between different batches of silicic magma is likely to have occurred (Gagnevin et al. 2005a, b), either in the source region or in the magma chamber (e.g., Mahood et al., 1996; Wiebe and Collins, 1998; Knesel et al., 1999).

7.3. Nature of end-members involved in mixing

These new Hf and O isotopic data on igneous and inherited/xenocrystic zircons (hereafter named ‘older zircons’) provide new constraints on the nature of the magma sources involved in the genesis of plutonic and volcanic rocks in the Tuscan archipelago.

Isotopic analyses of inherited zircon cores in granitic rocks, in conjunction with zircon analyses in putative metasedimentary source rocks, can potentially yield important clues on the nature of the crustal peraluminous component(s) involved in magma mixing. Older zircons have a wide range of ages (from 2852 Ma to 443 Ma; **Table** 1) and Hf isotopic composition. The Hf isotopic data indicate that at least three crustal components (with $\varepsilon Hf_{(t)}$ ~ 4.5, ~ 20-25 and ~ 60-70 epsilon units; **Electronic** Supplementary Material E) have intervened in the genesis of the Tuscan igneous rocks, either as magma sources or contaminants. O isotopic data on older zircon are scarce, but a range in $\delta^{18}O_{Zc}$ (from 10.3‰ to 17.9‰; **Fig**. 5b; **Electronic** Supplementary Material F) is also observed. No distinct Hf and O isotopic signatures arise whether the older zircons occur as inherited cores or as xenocrysts. Inherited cores and their magmatic overgrowths display large difference in $^{176}Hf/^{177}Hf$ ratios, implying prevalent open-system conditions.

Following Valley et al. (1994), $\delta^{18}O_{Zc}$ can be directly translated to $\delta^{18}O$ in the host melt ($\delta^{18}O_{melt}$). The study of Trail et al. (2009), which examined experimentally the extent of oxygen isotopic fractionation between zircon and melts of variable composition, enabled us to extrapolate the $\delta^{18}O_{melt}$ values at a given temperature of 800°C (i.e., average temperature for the Monte Capanne pluton; see Gagnevin et al., 2004). A zircon-melt fractionation factor of about 1.8 was obtained and applied to all $\delta^{18}O_{Zc}$ data (**Fig**. 5b). Most of the $\delta^{18}O_{melt}$ data plot within a narrow range of ca. 11 to 13‰, which also corresponds to most of the whole-rock $\delta^{18}O$ data in plutonic rocks from Tuscany (Taylor and Turri, 1976; **Fig**. 5b), and coincide, though only in part, with the older inherited zircon data (**Fig**. 5b). Overall, the zircon O isotope zircon data support large scale hybridisation within the entire archipelago, possibly in deep hot crustal zone (Annen et al., 2006; Kemp et al., 2006; Shaw and Flood, 2009) whereby efficient mixing between anatectic and mantle-derived melts occurred, a conclusion in line with the Hf isotopic results (**Fig**. 5a, 6).

As far as this study is concerned, the rim of the zircon grains DG264-7 in Giglio ($^{176}Hf/^{177}Hf = 0.28219$; not analysed for $\delta^{18}O$) and DG23-38 (with inherited core having a discordant age and high U-rim) in Porto Azzurro ($\delta^{18}O_{melt}$ = 21.4‰; $^{176}Hf/^{177}Hf$ = 0.28246) may be representative of the Hf and O isotopic compositions of the peraluminous magma end-members involved in magma mixing. Both grains have an inherited core, further corroborating this conclusion. The Hf signature of the rim of grain DG264-7 is in fact similar to many older grain cores occurring in Elba (**Electronic** Supplementary Material E). Generally, the extremely unradiogenic Hf signature of most of older zircons is compatible with a metasedimentary source, which may have undergone previous melt extraction events. On-going work on zircons from metasedimentary rocks in Elba is aiming to better constrain possible source rocks and the relevance of zircon inheritance in the Elba igneous complex, and elsewhere in the archipelago.

Our zircon trace element and isotopic data support the inference that Capraia-like metaluminous magmas were involved in the genesis of the plutonic rocks through magma mixing (Poli, 1992; Dini et al., 2002; Gagnevin et al., 2004; 2005a; 2005b). Compared with the plutonic rocks, the Capraia zircons display relatively simple textures (**Fig**. 2f) and limited variation in trace elements (Gagnevin et al., 2010) and isotopic compositions (weighted mean $^{176}Hf/^{177}Hf = 0.28260 \pm 0.00002$, n = 12; weighted mean $\delta^{18}O_{Zc} = 6.82 \pm 0.23‰$, n = 12). While $\delta^{18}O$ in Capraia is lower than in the plutonic rocks, its zircon Hf isotopic composition clearly overlaps with theirs (**Fig.** 5).

The peculiar, crustal-like, Hf and O isotopic nature of the Capraia zircons raises the possibility that a supracrustal component intervened in Capraia magmatism, which can be accounted for by the following four hypotheses:

1) The original mantle-derived magma was thoroughly contaminated by metasedimentary rocks.
2) Capraia magmatism derives from melting of metasedimentary rocks, that is, plutonic and volcanic rocks have the same origin, but result from different magma dynamics (residual melts vs. cumulate).
3) Thorough mixing between crustal and mantle-derived magmas occurred in Capraia and obliterated the original Hf and O signature of the mantle parent (e.g., Griffin et al., 2002).
4) Capraia volcanism derives from melting of lithospheric mantle enriched by subduction-related metasomatic agents.

The lack of physical evidence for contamination in Capraia, such as occurrence of crustal xenoliths, common in the plutonic counterpart (Westerman et al., 1993; Gagnevin et al., 2004), the absence of minerals typical of crustal inheritance (such as garnet, sillimanite, cordierite; Zeck and Williams, 2002; Kemp et al., 2006) and/or apparent absence of inherited zircon cores or xenocrysts suggest that crustal contamination or magma derivation from a metasedimentary source are unlikely to be the cause for the unradiogenic Hf and elevated $\delta^{18}O_{Zc}$ isotopic signatures of the Capraia zircons, hence ruling out hypotheses 1 and 2.

Hypothesis 3 may explain the striking similarity in $^{176}Hf/^{177}Hf$ between volcanic (largely mantle-derived) and plutonic (largely crustal-derived) rocks. However, we consider this hypothesis unlikely because of the lack of textural (e.g., no quartz xenocrysts) and geochemical (e.g., similar Sr and Nd isotopic ratios) evidence for thorough mixing between felsic peraluminous and mafic metaluminous magmas in Capraia. Instead, Capraia and Elba magmatic rocks preserve marked petrographic and geochemical differences (Poli and Perugini, 2003; Gagnevin et al., 2007).

Hypothesis 4 is attractive because there is a general consensus that the source of mantle-derived magmas in the Tuscan Magmatic Province has been severely modified by fluid-assisted metasomatism of supracrustal origin resulting from subduction of the Adriatic plate below the Italian peninsula (Vollmer, 1977; Hawkesworth and Vollmer, 1979; Peccerillo, 1999; Conticelli et al., 2002; 2009; Prelevic et al., 2008; 2010). Elevated $\delta^{18}O$, such as observed in this study, may be related to mantle metasomatism (Eiler et al., 1998), as also inferred from other magmatic ultrapotassic rocks in Central Italy (Ferrara et al., 1986; Frezzoti et al., 2007). Similarly, unradiogenic Hf is a common signature of ultrapotassic, lamproitic rocks in the Tuscan Magmatic province (with $^{176}Hf/^{177}Hf$ ratios down to 0.28240; **Fig**. 5a; Prelevic et al., 2010). Generally, our zircon Hf data rocks span the range of Hf isotopic composition exhibited by the Italian lamproitic rocks (**Fig**. 5a).

Lamproitic rocks provide important insights into metasomatic processes in the source of Tuscan magmatism (Conticelli, 1998; Peccerillo, 1999; Conticelli et al., 2009). The Capraia lavas also display petrographic evidence for mixing involving lamproitic magmas (occurrence of phlogopite, amphibole, sanidine), concurring with the relatively radiogenic Sr isotopic composition in both plagioclase and bulk rocks (Gagnevin et al., 2007), strong enrichment in incompatible elements (Poli and Perugini, 2003), as well as clinopyroxene chemical and structural data (Chelazzi et al., 2006). We note that Capraia lavas 1) do not display the high K_2O (> 7 wt%) and MgO (> 8 wt%) common to lamproitic rocks from Italy and generally worldwide (e.g., Davies et al., 2006), and 2) display more radiogenic Hf composition compared to typical lamproitic magmatism occurring in the western Mediterranean region (Prelevic et al., 2010). The mantle-derived end-member, inferred to be similar to Capraia magmatism, was thus not 'purely' lamproitic in origin, but was likely to be hybrid between lamproitic (unradiogenic $^{176}Hf/^{177}Hf$ signature) and high-K calc-alkaline (radiogenic $^{176}Hf/^{177}Hf$ signature) magmas. This implies that the veined lithospheric mantle source, contaminated with subducted crustal material (which melting produced lamproitic melts; Conticelli et al., 2002; Prelevic et al., 2008), was diluted by a large addition of fresh asthenospheric melts derived from the convecting mantle (Lustrino et al., 2011). Generally, mixing between different components within the mantle sources is thought to be important in the genesis of lamproitic magmas within the Mediterranean region (Prelevic et al., 2010), and is shown to be relevant to explain the Hf isotopic data of the Capraia zircons, and to some extent, the genesis of silicic magmatism in Tuscany. The overall range in $\delta^{18}O$ in Capraia zircons, sometimes observed at the intra-grain scale (**Fig**. 2f), is also interpreted as resulting from variable contribution of lamproitic-like melts in the erupted magma products.

8. Conclusions

The petrogenesis of igneous rocks in the Tuscan Archipelago has been investigated in this study using *in-situ* U-Pb, O and Hf isotopic analyses of zircon. Here, dacite (Capraia) and granitoids (Elba, Giglio) define almost continuous igneous activity over c. 3 Ma. This study is a rare example of the application of in-situ methods to explore the relationships between extrusive and intrusive magmatism as well as the nature of the components involved in their genesis. Particular emphasis has been placed on the Monte Capanne plutonic system for which a wealth of chemical and isotopic data is now available (Dini et al., 2002; Gagnevin et al., 2004; Gagnevin et al., 2005a,b). U-Pb zircon ion microprobe analyses indicate that igneous activity in Elba (including the Monte Capanne and Porto Azzurro pluton) occurred between 8.3 and 6.3 Ma, which overlapped with volcanic activity in Capraia (7.1-7.6 Ma). The presence of antecrystic zircon in the MC plutonic system suggests that construction of the MC pluton occurred over a period of c. 0.5 Ma, which overlaps with volcanic activity in Capraia. These data also indicate that the progressive assembly of pluton-forming magma batches in Elba occurred over a period of at least 2 Ma. The important role of magma mixing in the genesis of Tuscan igneous rocks has been emphasised in many petrological studies (Gagnevin et al., 2005a, and references therein). These new zircon U-Pb data suggest that hybridisation in Tuscan intrusive rocks took place over a period of ca. 3 Ma, whilst maintaining a similar Hf isotopic composition. We suggest that this similarity is fundamentally inherited from the nature of the mantle-derived magma, which provided the heat source in generating anatectic peraluminous magmas.

The range in zircon Hf and O isotopic composition (of ~7 Hf epsilon units and ~5‰, respectively) and the negative correlation between $\delta^{18}O$ and $^{176}Hf/^{177}Hf$ (**Fig**. 5) are indicative of some open-system behaviour involving several magma end-members in the genesis of the intrusive rocks, with a minor role for crustal contamination. In particular, these data provide clear evidence that mixing between several felsic end-members has occurred. As a corollary, we believe that any attempt to quantify the relative amount of end-members (mafic vs. silicic) by simple mixing calculations would be meaningless.

Our zircon isotopic data provide important insights into magma processes as well as the nature of the magma components involved in mixing. Generally, inherited/xenocrystic grains are scarce in Elba, but may point to the nature of the felsic peraluminous magmas involved in mixing. Older zircons display a large range in Hf (4 to 70 epsilon units) and O (10 to 18‰) isotopes, suggesting that several peraluminous magmas may have contributed to the Tuscan magmatism, either as magma sources or as contaminants.

Capraia magmatism represents the closest approach to the mantle-derived magma involved in mixing. The relatively unradiogenic Hf (mean $^{176}Hf/^{177}Hf = 0.28260$) and heavy $\delta^{18}O$ (5.9-7.5‰) in the Capraia zircons, neither of which is typical of mantle-derived magmas ($\delta^{18}O$ mantle ~5-5.5‰), imply that a crustal component was involved in the mantle source, probably as a result of metasomatism. On the basis of other petrological studies on the Tuscan Magmatic Province, our zircon data provide further evidence of a lamproitic origin for the Capraia magmatism, mixed with a significant amount of fresh asthenospheric melts. Hf isotopic data suggest that this signature is also recorded in the plutonic realm through magma mixing.

In situ isotopic measurements on zircons are thus excellent tools to unravel complex magmatic histories. However, we emphasise that using zircon Hf isotopic alone as a tracer of magmatic processes may be misleading unless it is done in conjunction with other geochemical tracers, such as oxygen isotopes.

Acknowledgments

This research was supported by Science Foundation Ireland (SFI) grant 04/BR/ES0007 awarded to JSD. We thank Dragan Prelevic and an anonymous reviewer as well as editor Rick Carlson for helpful reviews and comments that greatly improved the paper. We also thank Giampiero Poli for his support during fieldwork in Elba and Capraia, and Andreas Kronz for assistance with electron microprobe analyses. This paper is NORDSIM contribution number 2XX.

References

Aldighieri, B., Gamba, A., Groppelli, G., Malara, F., Pasquare, G., Testa, B., and Wijbrans, J., 1998. Methodology for the space-time definition of lateral collapse: the evolution model of Capraia Island (Italy). In: Buccianti A., Nardi G. Potenza R. (eds), Proceedings of IAMG '98, the Fourth Annual Conference of the International Association of Mathematical Geology, pp. 79-85.

Annen, C., Blundy, J.D., Sparks, R.S.J., 2006. The genesis of intermediate and silicic magmas in deep crustal hot zones. Journal of Petrology 47, 505-539.

Appleby, S.K., Graham, C.M., Gillespie, M.R., Hinton, R.W., Oliver, G.J.H., 2008. A cryptic record of magma mixing in diorites revealed by high-precision SIMS oxygen isotope analysis of zircons. Earth and Planetary Science Letters 269, 105–117.

Bachmann, O., Miller, C.F., de Silva, S.L., 2007. The volcanic-plutonic connection as a stage for understanding crustal magmatism. Journal of Volcanology and Geothermal Research 167, 1-23.

Belousova, E.A., Griffin, W.L., O'Reilly, S.Y., 2006. Zircon crystal morphology, trace element signatures and Hf isotope composition as a tool for petrogenetic modelling: Examples from Eastern Australian granitoids. Journal of Petrology 47, 329-353.

Blichert-Toft, J, Albarede, F., 1997. The Lu–Hf isotope geochemistry of chondrites and the evolution of the mantle-crust system. Earth and Planetary Science Letter 148, 243–258.

Boccaletti, M., Gianelli, G., Sani, F., 1997. Tectonic regime, granite emplacement and crustal structure in the inner zone of the Northern Appenines (Tuscany, Italy): a new hypothesis. Tectonophysics 270, 127-143.

Bolhar, R., Weaver, S.D., Whitehouse, M.J., Palin, J.M., Woodhead, J.D., Cole, J.W., 2008. Sources and evolution of arc magmas inferred from coupled O and Hf isotope systematics of plutonic zircons from the Cretaceous Separation Point Suite (New Zealand). Earth and Planetary Science Letters 268, 312-324.

Brunet, C., Monié, P., Jolivet, L., Cadet, J.P., 2000. Migration of compression and extension in the Tyrrhenian Sea, insights from $^{40}Ar/^{39}Ar$ ages on micas along a transect from Corsica to Tuscany. Tectonophysics 321, 127-155.

Butera, K.M., Williams, I.S., Blevin, P.L., Simpson, C.J., 2001. Zircon U-Pb dating of Early Palaeozoic monzonitic intrusives from the Goonumbla area, New South Wales. Australian Journal of Earth Sciences 48, 457-464.

Chelazzi, L., Bindi, L., Olmi, F., Menchetti, S., Peccerillo, A., Conticelli, S., 2006. A lamproitic component in high-K calc-alkaline volcanic rocks of the Capraia Island:

evidence from clinopyroxene crystal chemical data. Periodico di Mineralogia 75, 161-180.

Chu, M.F., Chung, S.L., Song, B.A., Liu, D.Y., O'Reilly, S. Y., Pearson, N.J., Ji, J.Q., Wen, D.J., 2006. Zircon U-Pb and Hf isotope constraints on the Mesozoic tectonics and crustal evolution of southern Tibet. Geology 34, 745-748.

Coleman, D.S., Gray, W., Glazner, A.F., 2004. Rethinking the emplacement and evolution of zoned plutons: Geochronologic evidence for incremental assembly of the Tuolumne Intrusive Suite, California. Geology 32, 433–436

Conticelli, S., 1998. The effect of crustal contamination on ultrapotassic magmas with lamproitic affinity: mineralogical, geochemical and isotope data from the Torre Alfina lavas and xenoliths, Central Italy. Chemical Geology 149, 51-81.

Conticelli, S., Bortolotti, V., Principi, G., Laurenzi, M.A., D'Antonio, M., Vaggelli., G. 2001. Petrology, mineralogy and geochemistry of a mafic dyke from Monte Castello, Elba Island, Italy. Ofioliti 26, 249-262.

Conticelli, S., D'Antonio, M., Pinarelli, L., Civetta, L., 2002. Source contamination and mantle heterogeneity in the genesis of Italian potassic and ultrapotassic volcanic rocks: Sr-Nd-Pb isotope data from Roman Province and Southern Tuscany. Mineralogy and Petrology 74, 189-222.

Conticelli, S., Guarnieri, L., Farinelli, A., Mattei, M., Avanzinelli, R., Bianchini, G., Boari, E., Tommasini, S., Tiepolo, M., Prelevic, D., Venturelli, G., 2009. Trace elements and Sr-Nd-Pb isotopes of K-rich, shoshonitic, and calc-alkaline magmatism of the Western Mediterranean Region: Genesis of ultrapotassic to calc-alkaline magmatic associations in a post-collisional geodynamic setting. Lithos 107, 68-92.

Daly, J.S., Gagnevin, D., Whitehouse, M.J., Horstwood, M.E, 2007. Zircon growth and resorption in an incrementally filled granite pluton: insights from in-situ U-Pb, trace element and Hf isotopic analyses. Geochimica et Cosmochimica Acta 71, A302.

Davies, G.R., Stolz, A.J., Mahotkin, I.L., Nowell, G.M., Pearson, D.G., 2006. Trace element and Sr-Pb-Nd-Hf isotope evidence for ancient, fluid-dominated enrichment of the source of Aldan shield lamproites. Journal of Petrology 47, 1119-1146.

Dini, A., Innocenti, F., Rocchi, S., Tonarini, S., Westerman, D.S., 2002. The magmatic evolution of the late Miocene laccolith-pluton-dyke granitic complex of Elba Island, Italy. Geological Magazine 139, 257-279.

Dini, A., Rocchi, S., Westerman, D.S., 2004. Reaction microtextures of REE-Y-Th-U accessory minerals in the Monte Capanne pluton (Elba Island, Italy): a possible indicator of hybridization processes. Lithos 78, 101-118.

Dini, A., Westerman, D.S., Innocenti, F, Rocchi, S., 2008. Magma emplacement in a transfer zone: the Miocene mafic Orano dyke swarm of Elba Island, Tuscany, Italy. In Thomson, K. and Petford, N. (eds) Structure and Emplacement of High-Level Magmatic Systems. Geological Society, London, Special Publications 302, 131–148.

Eiler, J.M., McInnes, B., Valley, J.W., Graham, C.M., Stolper, E.M., 1998. Oxygen isotope evidence for slab-derived fluids in the sub-arc mantle. Nature 393, 777-781.

Ferrara, G., Tonarini, S., 1985. Radiometric geochronology in Tuscany: results and problems. Rendiconti della Societá Italiana di Mineralogia e Petrologia 40, 111-124.

Ferrara, G., Preitemartinez, M., Taylor, H.P., Tonarini, S., Turi, B., 1986. Evidence for crustal assimilation, mixing of magmas, and a Sr-87-rich upper mantle - an oxygen and Strontium Isotope Study of the M. Vulsini volcanic area, Central Italy. Contributions to Mineralogy and Petrology 92, 269-280.

Flowerdew, M.J., Millar, I L., Vaughan, A.P.M., Horstwood, M.S.A., Fanning, C.M., 2006. The source of granitic gneisses and migmatites in the Antarctic Peninsula: a combined U-Pb SHRIMP and laser ablation Hf isotope study of complex zircons. Contributions to Mineralogy and Petrology 151, 751-768.

Gagnevin, D., 2005. Mineral- and whole-rock investigation of granite petrogenesis in a young plutonic system: the Monte Capanne pluton. PhD thesis, University College, Dublin.

Gagnevin, D., Daly, J.S., Poli, G., 2004. Petrographic, geochemical and isotopic constraints on magma dynamics and mixing in the Miocene Monte Capanne monzogranite (Elba Island, Italy). Lithos 78, 157-195.

Gagnevin, D., Daly, J.S., Poli, G., Morgan, D., 2005a. Microchemical and Sr isotopic investigation of zoned K-feldspar megacrysts: insights into the petrogenesis of a granitic system and disequilibrium processes during crystal growth. Journal of Petrology 46, 1689-1724.

Gagnevin, D., Daly, J.S., Waight, T., Morgan, D., Poli, G., 2005b. Pb isotopic zoning of K-feldspar megacrysts determined by laser ablation multiple-collector ICP-MS: insights into granite petrogenesis. Geochimica et Cosmochimica Acta 69, 1899-1915.

Gagnevin, D., Waight, T.E., Daly, J.S., Poli, G. Conticelli, S., 2007. Insights into magmatic evolution and recharge history in Capraia Volcano (Italy) from chemical and isotopic zoning in plagioclase phenocrysts. Journal of Volcanology and Geothermal Research 168, 28-54

Gagnevin, D., Daly, J.S., Poli, G., 2008a. Insights into granite petrogenesis from quantitative assessment of the field distribution of enclaves, xenoliths and K-feldspar megacrysts in the Monte Capanne pluton, Italy. Mineralogical Magazine 72, 925-940.

Gagnevin, D, Daly, J.S., Whitehouse, M.J., Horstwood, M., Kronz, A., 2008b. Zircon as Proxy of Magma Differentiation and Mixing in the Tuscan Magmatic Province (Italy). Goldschmidt Conference Abstracts, A288.

Gagnevin, D., Daly, J.S., Kronz., A., 2010. Zircon texture and chemical composition as a guide to magmatic processes and mixing in a granitic environment and coeval volcanic system. Contributions to Mineralogy and Petrology 159, 579-596.

Giraud, A., Dupuy, C., Dostal, J., 1986. Behaviour of trace elements during magmatic processes in the crust: application to acidic volcanic rocks of Tuscany (Italy). Chemical Geology 57, 269-288.

Glazner, A.F., Bartley, J.M., Coleman, D.S., Gray, W., Taylor, R.Z., 2004. Are plutons assembled over millions of years by amalgamation from small magma chambers? GSA Today 14, 4–11

Griffin, W.L., Pearson, N.J., Belousova, E., Jackson, S.E., van Achterbergh, E., O'Reilly, S.Y., Shee, S.R., 2000. The Hf isotope composition of cratonic mantle: LAM-MC-ICPMS analysis of zircon megacrysts in kimberlites. Geochimica et Cosmochimica Acta 64, 133-147.

Griffin, W.L., Wanga, X., Jackson, S.E., Pearson, N J., O'Reilly, S.Y., Xua, X., Zhouc, X., 2002. Zircon chemistry and magma mixing, SE China: In-situ analysis of Hf isotopes, Tonglu and Pingtan igneous complexes. Lithos 61, 237-269.

Harley, S.L., Kelly, N.M., 2007. Zircon: Tiny but Timely. Elements 3(1), 1-80.

Hawkesworth, C.J., Vollmer, R., 1979. Crustal contamination versus enriched mantle: $^{143}Nd/^{144}Nd$ and $^{87}Sr/^{86}Sr$ evidence from the Italian volcanics. Contributions to Mineralogy and Petrology 69, 151-165.

Hawkesworth, C.J., Kemp, A.I.S. (2006. Using hafnium and oxygen isotopes in zircons to unravel the record of crustal evolution. Chemical Geology 226, 144–162.

Innocenti, F., Serri, G., Ferrara, G., Manetti, P., Tonarini, S., 1992. Genesis and classification of the rocks of the Tuscan Magmatic Province: thirty years after Marinelli's model. Acta Vulcanologica 2, 247-265.

Juteau, M., Michard, A.J., Albarède, F., 1984. Isotopic heterogeneities in the granitic intrusion of Monte Capanne (Elba Island, Italy) and dating concepts. Journal of Petrology 25, 532-545.

Kemp, A.I.S., Wormald, R.J., Whitehouse, M.J., Price, R.C., 2005. Hf isotopes in zircon reveal contrasting sources and crystallization histories for alkaline to peralkaline granites of Temora, southeastern Australia. Geology 33, 797-800.

Kemp, A.I.S., Hawkesworth, C J., Paterson, B.A., Foster, G.L., Kinny, P.D., Whitehouse, M.J., Maas, R., EIMF, 2006. Exploring the plutonic-volcanic link: a zircon U-Pb, Lu-Hf and O isotope study of paired volcanic and granitic units from southeastern Australia. Transactions of the Royal Society of Edinburgh-Earth Sciences 97, 337-355.

Kemp, A.I.S., Hawkesworth, C.J., Foster, G.L., Paterson, B.A., Woodhead, J.D., Hergt, J.M., Gray, C. M., Whitehouse, M J., 2007. Magmatic and crustal differentiation history of granitic rocks from Hf-O isotopes in zircon. Science 315(5814), 980-983.

Knesel, K.M., Davidson, J.P., and Duffield, W.A., 1999. Evolution of silicic magma through assimilation and subsequent recharge: Evidence from Sr isotopes in sanidine phenocrysts, Taylor Creek Rhyolite, NM. Journal of Petrology 40, 773-786.

Ludwig, K.R., 2003. User's Manual for Isoplot 3.00. A Geochronological Toolkit for Microsoft Excel. Berkeley Geochronology Center Special Publication No. 4, 70 pp.

Lustrino M., Duggen, S. and Rosenberg, C.L., 2011. The Central-Western Mediterranean: anomalous igneous activity in an anomalous collisional tectonic setting. Earth-Science Reviews 104, 1-40.

Mahood, G.A., Nibler, G.E., Halliday, A.N., 1996. Zoning patterns and petrologic processes in peraluminous magma chamber: Hall Canyon pluton, Panamint Mountains, California. GSA Bulletin 108, 437-453.

Matzel, J.E.P., Bowring, S.A., Miller, R.B., 2006. Time scales of pluton construction at differing crustal levels: Examples from the Mount Stuart and Tenpeak intrusions, North Cascades, Washington. Geological Society of America Bulletin 118, 1412–1430.

Miller, J.S., Matzel, J.E.P., Miller, C.F., Burgess, S.D., Miller, R.B., 2007. Zircon growth and recycling during the assembly of large, composite arc plutons. Journal of Volcanology and Geothermal Research 167, 282-299.

Nowell, G.M., Kempton, P.D., Noble, S.R., Fitton, J.G., Saunders, A.D., Mahoney, J.J., Taylor, R.N., 1998. High precision Hf isotope measurements of MORB and OIB by thermal ionisation mass spectrometry: insights into the depleted mantle. Chemical Geology 149, 211-233.

Peccerillo, A., 1999. Multiple mantle metasomatism in central-southern Italy: Geochemical effects, timing and geodynamic implications. Geology 27, 315-318.

Poli, G., 1992. Geochemistry of Tuscan Archipelago granitoids (Central Italy): the role of hybridization processes in their genesis. Journal of Geology 100, 41-56.

Poli, G., 2004. Genesis and evolution of Miocene-Quaternary intermediate-acid rocks from the Tuscan Magmatic province. Periodico di Mineralogia 73, 187-214.

Poli, G., Manetti, P., Tommasini, S., 1989. A petrological review on Miocene-Pliocene intrusive rocks from Southern Tuscany and Tyrrhenian Sea (Italy). Periodico di Mineralogia 58, 109-126.

Poli, G., Perugini, D., 2003. The Island of Capraia. In Miocene to recent plutonism and volcanism in the Tuscan Magmatic Province (Central Italy), ed. G. Poli, D. Perugini, S. Rocchi, and A. Dini. Periodico di Mineralogia, 72, 195-200

Prelevic, D., Foley, S.F., Romer, R., and Conticelli S., 2008. Mediterranean tertiary lamproites derived from multiple source components in postcollisional geodynamics. Geochimica Et Cosmochimica Acta 72(8), 2125-2156.

Prelevic, D., Stracke, A., Foley, S.F., Romer, R.L., Conticelli S., 2010. Hf isotope compositions of Mediterranean lamproites: Mixing of melts from asthenosphere and crustally contaminated mantle lithosphere. Lithos, 119(3-4), 297-312.

Principi, G., Treves, B., 1984. Il sistema corso-appenninico come prisma d'accrezione. Riflessi sul problema generale del limite Alpi-Appenini. Memoria della Societá Geologica Italiana 28, 549-576.

Reid, A., Wilson, C.J.L., Shun, L., Pearson, N., Belousova, E., 2007. Mesozoic plutons of the Yidun Arc, SW China: U/Pb geochronology and Hf isotopic signature. Ore Geology Reviews 31, 88-106.

Saupé, F., Marignac, C., Moine, B., Sonet, J., Zimmerman, J-L., 1982. Datation par les méthodes K/Ar et Rb/Sr de quelques roches de la partie orientale de l'Ile d'Elba (province de Livourne, Italie). Bulletin of Volcanology 105, 236-245.

Serri, G., Innocenti, F., Manetti, P., 1993. Geochemical and petrological evidence of the subduction of delaminated Adriatic lithosphere in the genesis of the Neogene-Quaternary magmatism of central Italy. Tectonophysics 223, 117-147.

Shaw, S.E., Flood, R.H., 2009. Zircon Hf Isotopic Evidence for Mixing of Crustal and Silicic Mantle-derived Magmas in a Zoned Granite Pluton, Eastern Australia. Journal of Petrology 50(1), 147-168.

Söderlund, U., Patchett, P.J., Vervoort, J.D., Isachsen, C.E., 2004. The ^{176}Lu decay constant determined by Lu–Hf and U–Pb isotope systematics of Precambrian mafic intrusions. Earth and Planetary Science Letters 219, 311–324.

Stacey, J.S., Kramers, J.D., 1975. Approximation of Terrestrial Lead Isotope Evolution by a 2-Stage Model. Earth and Planetary Science Letters 26, 207-221.

Taylor, H.P., Turi, B., 1976. High-^{18}O Igneous Rocks from the Tuscan Magmatic Province, Italy. Contributions to Mineralogy and Petrology 55, 33-54.

Trail, D., Bindeman, I.N., Watson, E.B., and Schmitt A.K., 2009. Experimental calibration of oxygen isotope fractionation between quartz and zircon. Geochimica Et Cosmochimica Acta 73(23), 7110-7126.

Valley, J.W., Chiarenzelli, J.R., McLelland, J.M., 1994. Oxygen isotope geochemistry of zircon. Earth and Planetary Science Letters 126, 187–206.

Valley, J.W., Kinny, P.D., Schulze, D.J., Spicuzza, M.J., 1998. Zircon megacrysts from kimberlite: oxygen isotope variability among mantle melts. Contributions to Mineralogy and Petrology 133, 1-11.

Vollmer, R., 1977. Isotopic evidence for genetic relations between acid and alkaline rocks in Italy. Contributions to Mineralogy and Petrology 60, 109-118.

Westerman, D.S., Innocenti, F., Tonarini, S., Ferrara, G., 1993. The Pliocene intrusions of the Island of Giglio. Memoria della Società Geologica Italiana 49, 345-363.

Whitehouse, M.J., Kamber, B.S., 2005. Assigning dates to thin gneissic veins in high-grade metamorphic terranes: a cautionary tale from Akilia, southwest Greenland. Journal of Petrology 46, 291–318.

Whitehouse M.J., Nemchin, A.A., 2009. High precision, high accuracy measurement of oxygen isotopes in a large lunar zircon by SIMS. Chemical Geology 261, 32-42.

Wiebe, R.A., Collins, W.J., 1998. Depositional features and stratigraphic sections in granitic plutons: implications for the emplacement and crystallisation of granitic magma. Journal of Structural Geology 20, 1273-1289.

Wiedenbeck, M., Alle, P., Corfu, F., Griffin, W. L., Meier, M., Oberli, F., Vonquadt, A., Roddick, J.C., Speigel, W., 1995. 3 Natural Zircon Standards for U-Th-Pb, Lu-Hf, Trace-Element and REE Analyses. Geostandards Newsletter 19, 1-23.

Wiedenbeck, M., Hanchar, J.M., Peck, W.H., Sylvester, P., Valley, J., Whitehouse, M., Kronz, A., Morishita, Y., Nasdala, L., Fiebig, J., Franchi, I., Girard, J.P., Greenwood, R.C., Hinton, R., Kita, N., Mason, P.R.D., Norman, M., Ogasawara, M., Piccoli, R., Rhede, D., Satoh, H., Schulz-Dobrick, B., Skar, O., Spicuzza, M.J., Terada, K., Tindle, A., Togashi, S., Vennemann, T., Xie, Q., Zheng, Y.F., 2004. Further characterisation of the 91500 zircon crystal. Geostandards and Geoanalytical Research 28, 9-39.

Woodhead, J., Hergt, J., Shelley, M., Eggins, S., Kemp, R., 2004. Zircon Hf-isotope analysis with an excimer laser, depth profiling, ablation of complex geometries, and concomitant age estimation. Chemical Geology 209, 121-135.

Woodhead, J.D., Hergt, J.M., 2005. A preliminary appraisal of seven natural zircon reference materials for in-situ Hf isotope determination. Geostandards and Geoanalytical Research 29, 183-195.

Yang, J.H., Wu, F.Y., Chung, S.L., Wilde, S.A., Chu, M.F., 2006. A hybrid origin for the Qianshan A-type granite, northeast China: Geochemical and Sr-Nd-Hf isotopic evidence. Lithos 89, 89-106.

Yang, J.H., Wu, F.Y., Wilde, S.A., Xie, L.W., Yang, Y.H., Liu, X.M., 2007. Tracing magma mixing in granite genesis: in-situ U-Pb dating and Hf-isotope analysis of zircons. Contributions to Mineralogy and Petrology 153, 177-190.

Zeck, H.P., Whitehouse, M.J., 2002. Pre-eruptional magmatic zircon, Neogene Alboran volcanic province, SE Spain. Journal of the Geological Society, London 159, 343-346.

Zeck, H.P., Williams, I.S., 2002. Inherited and magmatic zircon from Neogene Hoyazo cordierite dacite, SE Spain - Anatectic source rock provenance and magmatic evolution. Journal of Petrology 43, 1089-1104.

Figure captions:

Fig. 1: (a) Sketch map showing the magmatic centers constituting the Tuscan Magmatic Province (TMP); the approximate location of the Roman Magmatic province is also shown for comparison. The Tuscan Archipelago is composed of the islands of Giglio, Elba, Montecristo and Capraia. (b) Sketch map showing the Monte Capanne plutonic system (the most extensively studied intrusion in the archipelago; Gagnevin et al. (2005a) and references therein), with sample localities.–The subdivision between the Pomonte facies and the Sant' Andrea facies (**Fig**. 1b) is based on the distribution of K-feldspar megacrysts, xenoliths and mafic enclaves in the intrusion (Gagnevin et al., 2008a).

Fig. 2: Backscattered electron (BSE) images of representative zircon from Elba and Capraia. These BSE images were obtained using a JEOL 8900 RL electron microprobe at the Department of Geochemistry, 'Geowissenschafliches Zentrum der Universitat Göttingen' (GZG) (Gagnevin et al., 2010). Yellow circles indicate the location of LA-MC-ICPMS spots for Hf analysis (with $^{176}Hf/^{177}Hf$ ratio beside), blue circles indicate the location of ion microprobe spots for oxygen analysis (with $\delta^{18}O$ value beside), while the white ellipse in (c) represents the location of the ion microprobe U-Pb analyses. (a), (b): typical patchy-zoned zircon core, consisting of high U-Th-Y zircon (original) coexisting with low U-Th-Y zircon (replacement zircon); (c): homogenous zircon core in the MC monzogranite; (d): prominent oscillatory zoning occasionally punctuated by resorption zones in a zircon from granite porphyry DG259; (e) anhedral inherited core in DG220 (unpublished data from Daly and Gagnevin), followed by oscillatory zoning; (f): zircon texture typical of the Capraia dacite DG05-01, with little compositional contrast between core and rim. Reported errors for both O and Hf isotopic data are at 2σ sigma level.

Fig. 3: Summary of ion microprobe U-Pb ages obtained in this study. (a) Tera-Wasserburg concordia diagram for zircons from the Elba and Giglio plutonic samples (see Fig. 1); (b) Tera-Wasserburg concordia diagram for zircons in the Capraia volcanic sample DG05-1; Plotted uncertainties are 2σ.

Fig. 4: Weighted mean $^{206}Pb/^{238}U$ ages for a) Monte Capanne (MC) monzogranite and Orano dyke (OD), Monte Capanne plutonic system, Elba, excluding two analyses interpreted to be antecrystic (see text), b) Capraia dacite (five analyses excluded), c) Elba granite porphyry, d) Porto Azzurro granite, Elba and e) Giglio monzogranite. Samples and individual 2σ error bars are labeled as in Table 1. The main phase of zircon crystallisation in Capraia occurred around 7.3 Ma, i.e., similar to the MC pluton, though older and younger ages (Table 1) suggest protracted magmatism for at least 0.6 Ma.

Fig. 5: Cumulative probability plots for a) Hf and b) O isotopic variations for the samples investigated in this study, with reported in a) the whole-rock $^{176}Hf/^{177}Hf$ data for the Italian lamproites (see data from Prelevic et al; 2010) and in b) the whole-rock $\delta^{18}O$ data for the Tuscan igneous rocks (Taylor and Turi, 1976). Dashed line in diagram b) represents the calculated $\delta^{18}O$ value of the melt ($\delta^{18}O_{melt}$) following the experimental data of Trail et al. (2009) (see text for details). Uncertainties for individual measurements are at 2σ level. Insets in a) and b): range of Hf and O zircon data displayed by samples DG236 and DG314; data are arranged in order of increasing $^{176}Hf/^{177}Hf$ ratios and $\delta^{18}O$ for the two samples. These two samples exhibit a range of $^{176}Hf/^{177}Hf$ and $\delta^{18}O$ outside analytical uncertainty, indicative of open-system processes. We emphasise that it is likely to be the case for most of the other samples we have investigated (since similar textures were encountered; see **Fig**. 2; Gagnevin et al., 2010), but was simply not resolvable under our analytical conditions, especially for Hf. In diagram a), most of the inherited/xenocrytic grains are not plotted for scale reasons, as these display severely unradiogenic Hf compositions (see Electronic Supplementary Material E). In diagram b), the oxygen mantle values are from Eiler et al. (1998).

Fig. 6: Correlation between zircon $^{206}Pb/^{238}U$ ages and $^{176}Hf/^{177}Hf$ isotopic ratio in Tuscan magmatic rocks (reported error are 2σ). Note the similarity in Hf isotopic composition between the Elba granite porphyry (old) and the Giglio monzogranite (young), suggesting a common source throughout the magmatic evolution of the archipelago (c. 3 Ma), which we infer to be fundamentally related to a similar mantle parent as a trigger for anatexis.

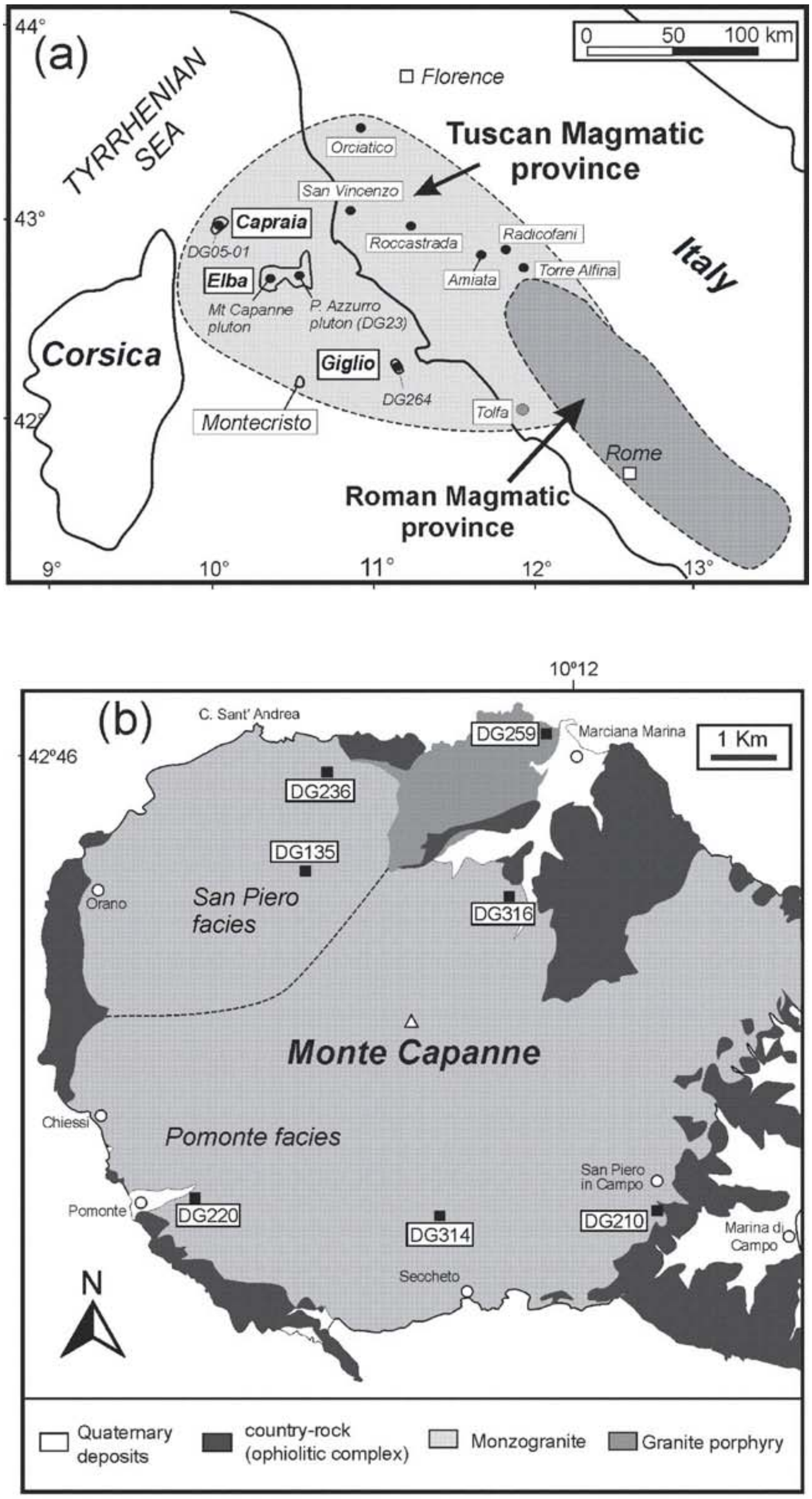
(a)
TYRRHENIAN SEA
Florence
0 50 100 km
Tuscan Magmatic province
Orciatico
San Vincenzo
Capraia
DG05-01
Roccastrada
Radicofani
Torre Alfina
Amiata
Italy
Elba
Mt Capanne pluton
P. Azzurro pluton (DG23)
Corsica
Giglio
DG264
Montecristo
Tolfa
Rome
Roman Magmatic province
44°
43°
42°
9°
10°
11°
12°
13°
(b)
10°12
42°46
C. Sant' Andrea
DG259
Marciana Marina
1 Km
DG236
DG135
Orano
San Piero facies
DG316
Monte Capanne
Chiessi
Pomonte facies
San Piero in Campo
Pomonte
DG220
DG314
DG210
Marina di Campo
Secchetto
N
Quaternary deposits
country-rock (ophiolitic complex)
Monzogranite
Granite porphyry

1022

Fig. 1

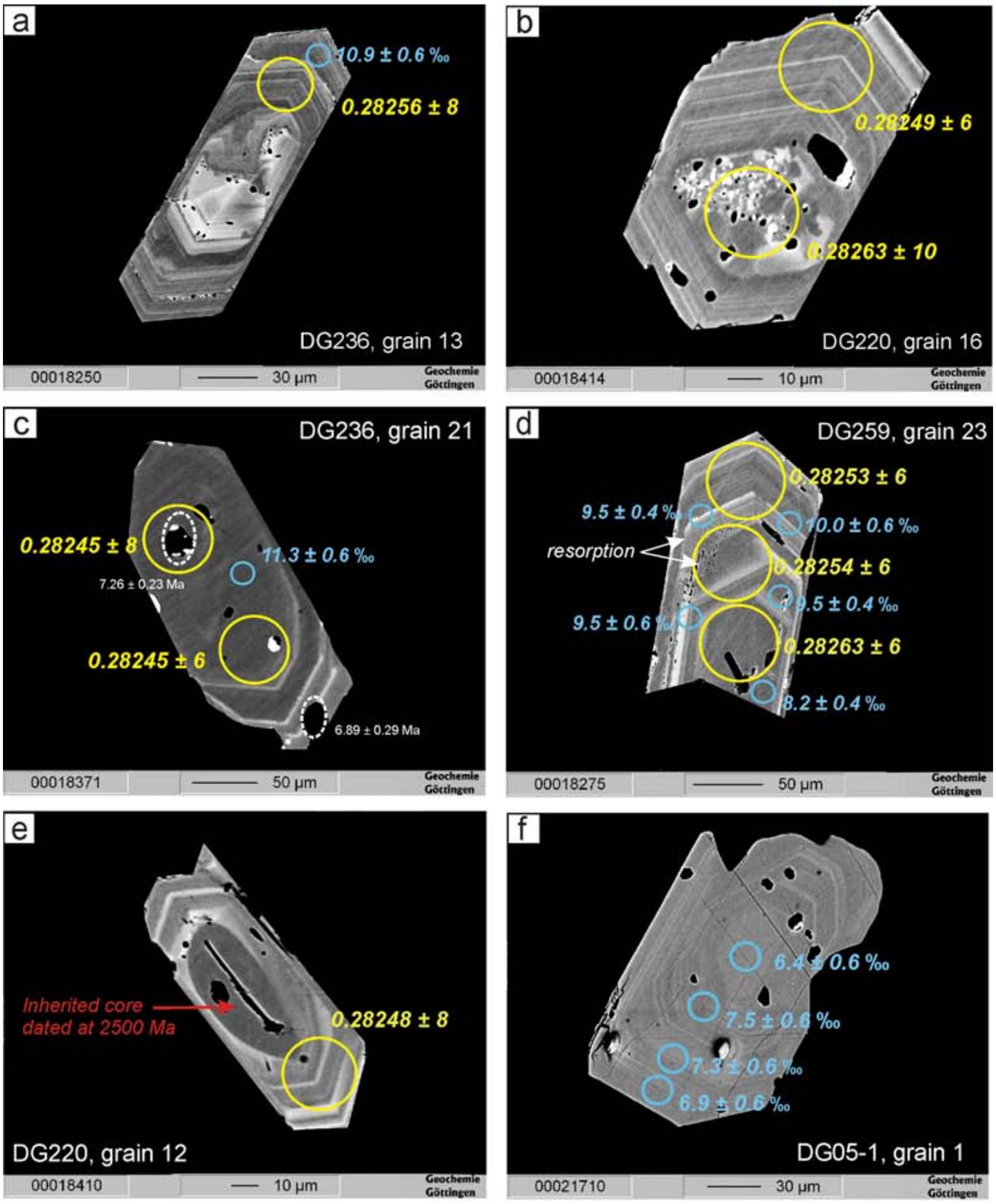
a
10.9 ± 0.6 ‰
0.28256 ± 8
DG236, grain 13
00018250
30 µm
Geochemie Göttingen
b
0.28249 ± 6
0.28263 ± 10
DG220, grain 16
00018414
10 µm
Geochemie Göttingen
c
DG236, grain 21
0.28245 ± 8
11.3 ± 0.6 ‰
7.26 ± 0.23 Ma
0.28245 ± 6
6.89 ± 0.29 Ma
00018371
50 µm
Geochemie Göttingen
d
DG259, grain 23
0.28253 ± 6
9.5 ± 0.4 ‰
10.0 ± 0.6 ‰
resorption
0.28254 ± 6
9.5 ± 0.4 ‰
9.5 ± 0.6 ‰
0.28263 ± 6
8.2 ± 0.4 ‰
00018275
50 µm
Geochemie Göttingen
e
Inherited core
dated at 2500 Ma
0.28248 ± 8
DG220, grain 12
00018410
10 µm
Geochemie Göttingen
f
6.4 ± 0.6 ‰
7.5 ± 0.6 ‰
7.3 ± 0.6 ‰
6.9 ± 0.6 ‰
DG05-1, grain 1
00021710
30 µm
Geochemie Göttingen

Fig. 2

1023

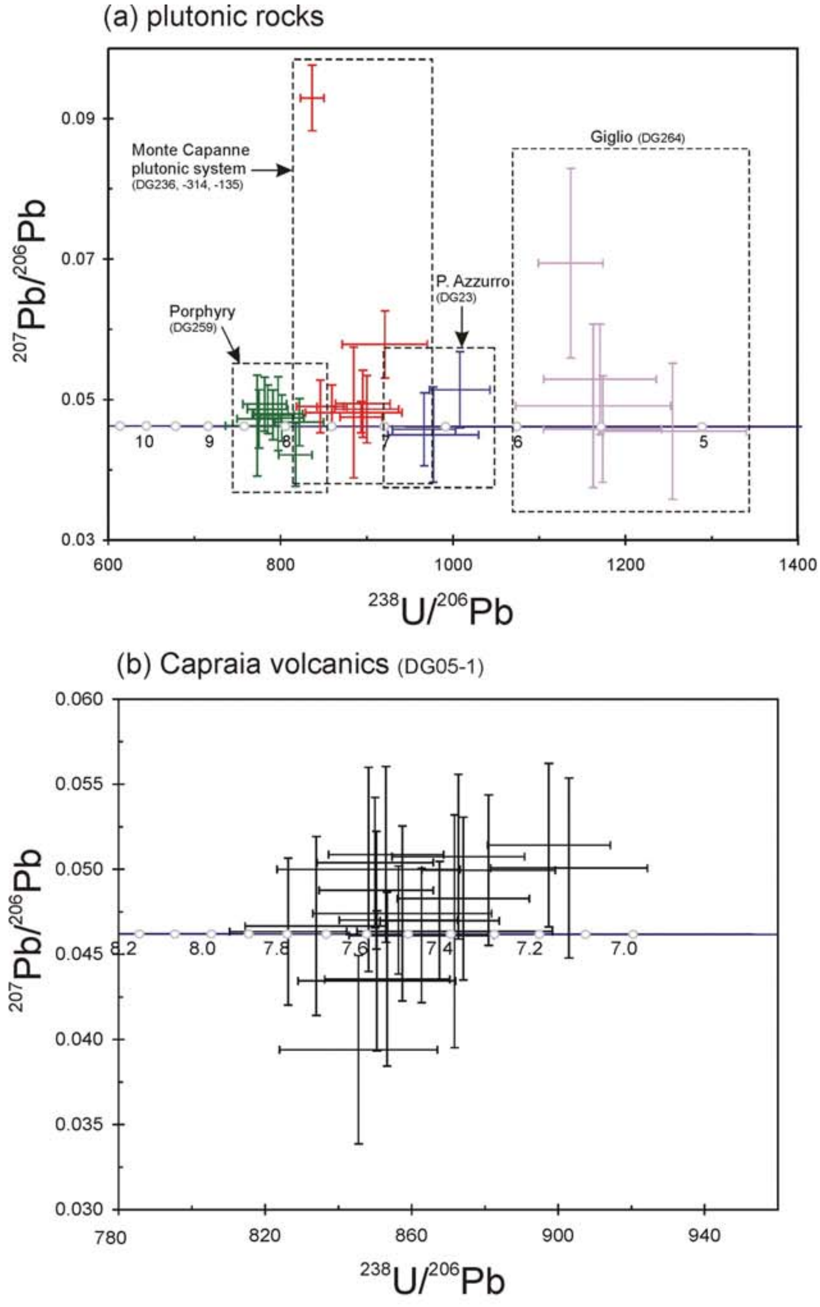
(a) plutonic rocks
Monte Capanne
plutonic system
(DG236, -314, -135)
Giglio (DG264)
P. Azzurro
(DG23)
Porphyry
(DG259)
0.09
0.07
0.05
0.03
10
9
8
7
6
5
600
800
1000
1200
1400
207Pb/206Pb
238U/206Pb
(b) Capraia volcanics (DG05-1)
0.060
0.055
0.050
0.045
0.040
0.035
0.030
8.2
8.0
7.8
7.6
7.4
7.2
7.0
780
820
860
900
940
207Pb/206Pb
238U/206Pb

Fig. 3

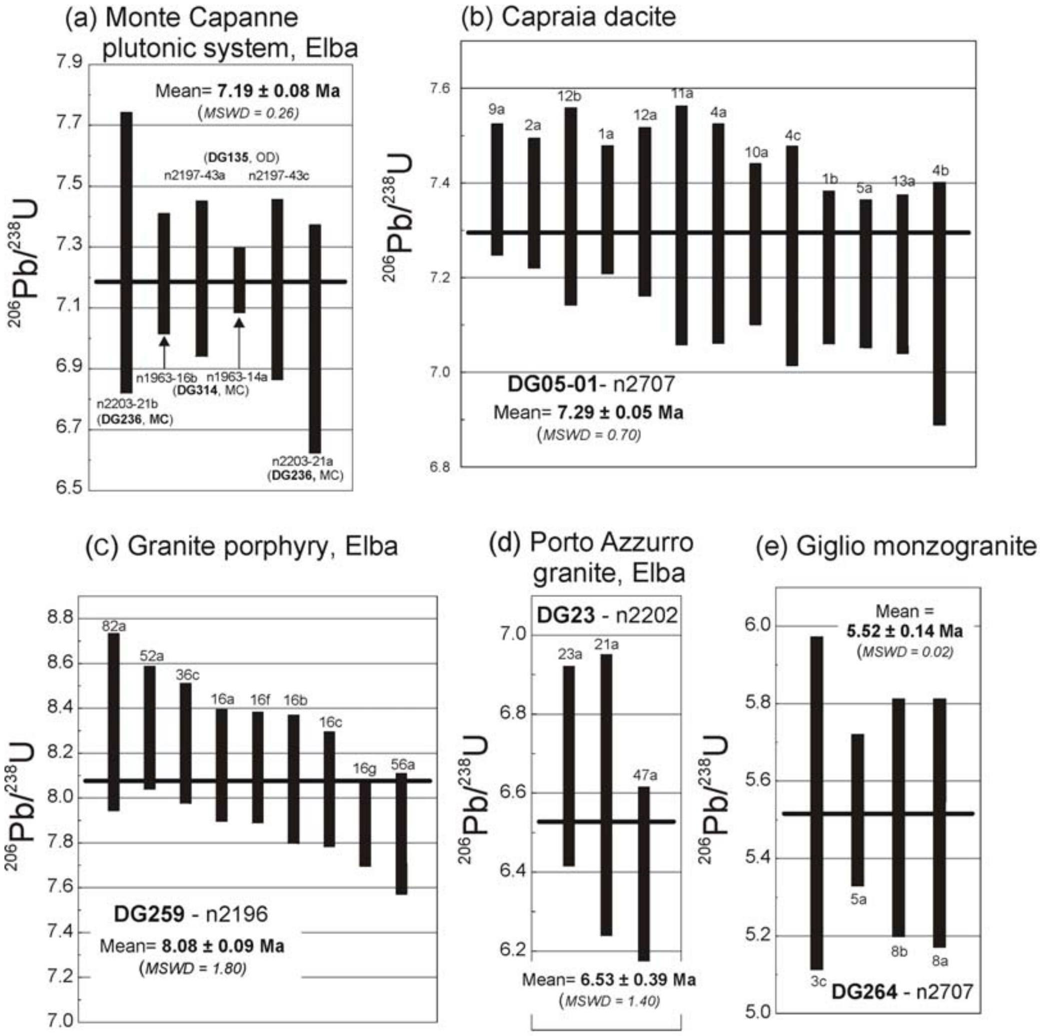
(a) Monte Capanne plutonic system, Elba
Mean= 7.19 ± 0.08 Ma
(MSWD = 0.26)
(DG135, OD)
n2197-43a
n2197-43c
n1963-16b
n1963-14a
(DG314, MC)
n2203-21b
(DG236, MC)
n2203-21a
(DG236, MC)
$^{206}Pb/^{238}U$
(b) Capraia dacite
9a
2a
12b
1a
12a
11a
4a
10a
4c
1b
5a
13a
4b
DG05-01- n2707
Mean= 7.29 ± 0.05 Ma
(MSWD = 0.70)
(c) Granite porphyry, Elba
82a
52a
36c
16a
16f
16b
16c
16g
56a
DG259 - n2196
Mean= 8.08 ± 0.09 Ma
(MSWD = 1.80)
(d) Porto Azzurro granite, Elba
DG23 - n2202
23a
21a
47a
Mean= 6.53 ± 0.39 Ma
(MSWD = 1.40)
(e) Giglio monzogranite
Mean = 5.52 ± 0.14 Ma
(MSWD = 0.02)
5a
8b
8a
3c
DG264 - n2707

1025 Fig. 4

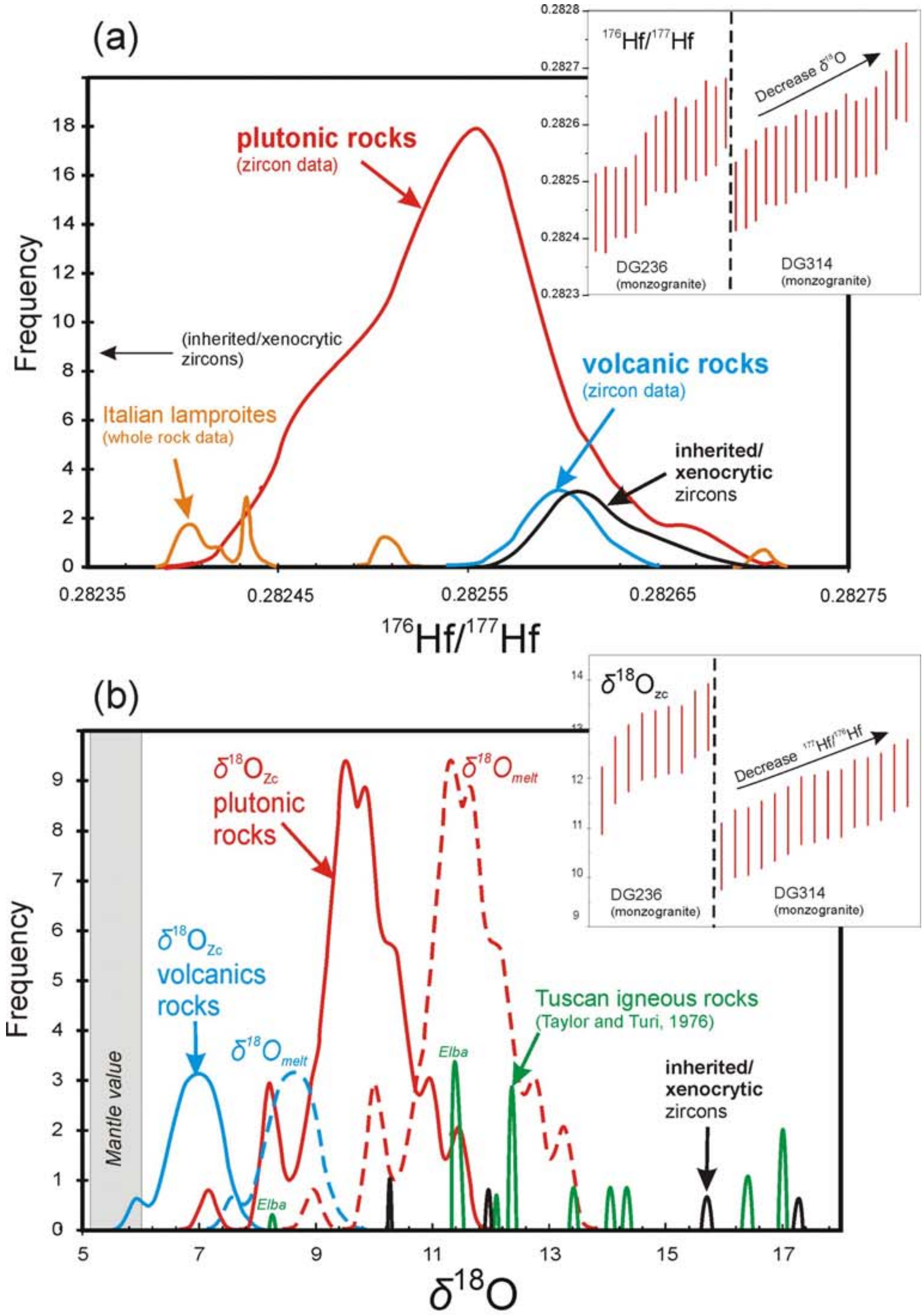
(a)
plutonic rocks
(zircon data)
Frequency
(inherited/xenocrytic
zircons)
Italian lamproites
(whole rock data)
volcanic rocks
(zircon data)
inherited/
xenocrytic
zircons
0.28235
0.28245
0.28255
0.28265
0.28275
$^{176}Hf/^{177}Hf$
$^{176}Hf/^{177}Hf$
Decrease $\delta^{18}O$
DG236
(monzogranite)
DG314
(monzogranite)
(b)
$\delta^{18}O_{Zc}$
plutonic
rocks
$\delta^{18}O_{melt}$
$\delta^{18}O_{Zc}$
volcanics
rocks
$\delta^{18}O_{melt}$
Mantle value
Elba
Tuscan igneous rocks
(Taylor and Turi, 1976)
inherited/
xenocrytic
zircons
$\delta^{18}O$
$\delta^{18}O_{zc}$
Decrease $^{177}Hf/^{176}Hf$
DG236
(monzogranite)
DG314
(monzogranite)

Fig. 5

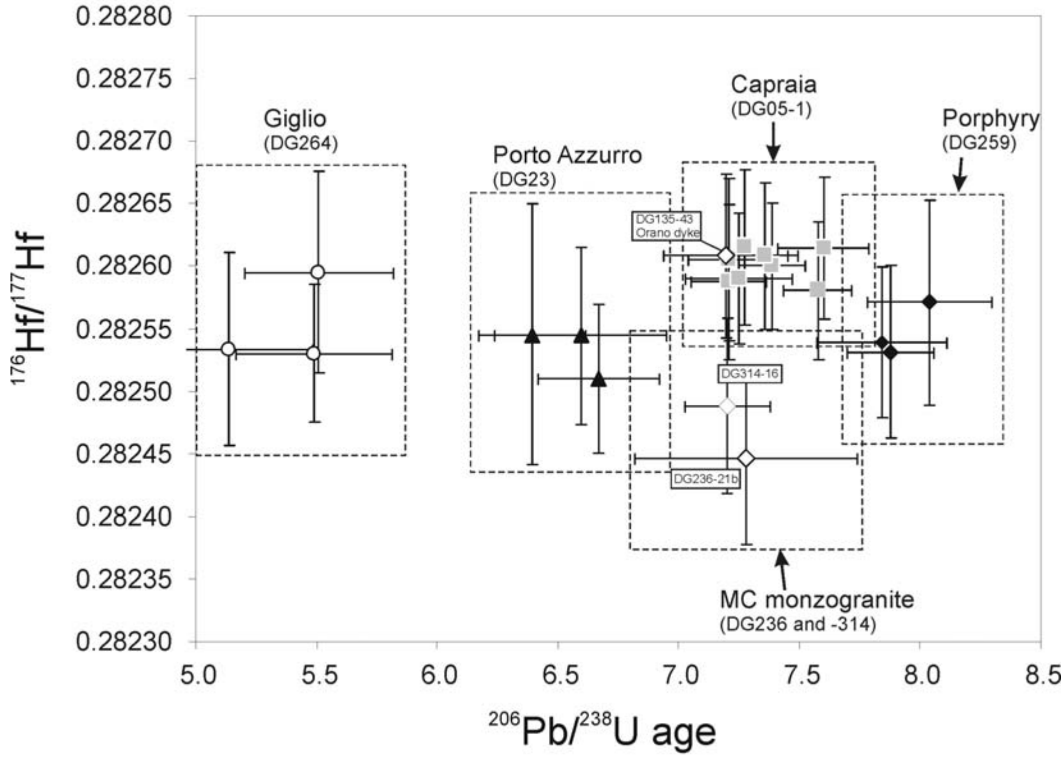
Giglio
(DG264)
Porto Azzurro
(DG23)
Capraia
(DG05-1)
Porphyry
(DG259)
DG135-43
Orano dyke
DG314-16
DG236-21b
MC monzogranite
(DG236 and -314)
$^{176}Hf/^{177}Hf$
$^{206}Pb/^{238}U$ age
0.28280
0.28275
0.28270
0.28265
0.28260
0.28255
0.28250
0.28245
0.28240
0.28235
0.28230
5.0
5.5
6.0
6.5
7.0
7.5
8.0
8.5

Fig. 6

Table 1: U-Pb ion microprobe analyses of magmatic and xenocrystic/inherited zircons from the Tuscan Archipelago.

analysis name	grain	comment	$^{238}U/^{206}Pb$	$\pm\sigma$	$^{207}Pb/^{206}Pb$	$\pm\sigma$	$^{206}Pb/^{238}U$ age (Ma)	$\pm 2\sigma$	207-corrected age (Ma)	$\pm 2\sigma$	U ppm	Th ppm	Pb ppm	f_{206}%
DG135 (Elba, MC plutonic system - Orano dyke)														
n2197-21b	21	rim	846	14	0.0490	0.0019	7.62	0.25	7.59	0.25	2361	751	3	{0.5}
n2197-43a	43	core	895	16	0.0494	0.0024	7.20	0.26	7.17	0.26	938	580	1	{0.7}
n2197-43c	43	rim	900	19	0.0486	0.0024	7.16	0.30	7.14	0.30	757	431	1	{0.5}
DG314 (Elba, MC plutonic system - monzogranite)														
n1963-14a	14	core	837	7	0.0929	0.0023	7.19	0.11	7.24	0.17	2535	956	3	6.63
n1963-16b	16	rim	893	12	0.0475	0.0011	7.21	0.20	7.20	0.20	2526	193	3	{0.27}
DG236 (Elba, MC plutonic system - monzogranite)														
n2203-4b	4	core	860	9	0.0490	0.0016	7.50	0.15	7.47	0.15	2798	254	4	{0.39}
n2203-21b	21	core	885	28	0.0482	0.0047	7.28	0.46	7.26	0.47	279	71	-	{3.61}
n2203-21a	21	rim	921	25	0.0579	0.0024	7.00	0.37	6.89	0.38	410	117	1	{2}
DG316 (Elba, MC plutonic system - monzogranite)														
n2198-29a	29	inher. core	8.3	0.1	0.066	0.001	730	12	-		241	129	36	{0.04}
n2198-33a	33	inher. core	10.2	0.1	0.061	0.000	600	10	-		614	813	87	{0.02}
n2198-24a	24	inher. core	10.2	0.1	0.060	0.000	606	9	-		320	171	39	{0.03}
n2198-23a	23	xenocryst	3.9	0.0	0.120	0.001	1455	22	-		199	158	70	{0.01}
n2198-28a	28	xenocryst	2.3	0.0	0.175	0.001	2341	34	-		135	36	74	{0.01}
n2198-50a	50	xenocryst	3.1	0.0	0.114	0.001	1801	25	-		325	168	133	{0.01}
n2198-59a	59	xenocryst	6.9	0.2	0.070	0.001	874	51	-		103	52	19	{0.00}
DG220 (Elba, MC plutonic system - mafic microgranular enclave)														
n2200-45a	45	inher. core	10.0	0.1	0.065	0.001	612	9	-		146	52	17	{0.05}
n2200-44a	44	xenocryst	14.1	0.1	0.056	0.000	443	7			521	66	40	{0.01}
DG259 (Elba, granite porphyry)														
n2196-16a	16	core	791	12	0.0478	0.0018	8.15	0.25	8.13	0.25	2208	521	3	{0.5}
n2196-16c	16	core	801	13	0.0474	0.0016	8.04	0.26	8.03	0.26	2063	416	3	{0.5}
n2196-16b	16	core	797	14	0.0480	0.0026	8.08	0.29	8.06	0.29	1196	160	2	{0.0}
n2196-16f	16	core	785	12	0.0486	0.0017	8.14	0.25	8.18	0.25	2581	385	4	0.9
n2196-16g	16	core	817	10	0.0421	0.0022	7.88	0.19	7.92	0.19	1359	175	2	{0.5}
n2196-36c	36	core	782	13	0.0494	0.0019	8.24	0.27	8.21	0.27	1881	1021	3	{0.72}
n2196-52a	52	core	775	13	0.0473	0.0021	8.31	0.27	8.30	0.28	1075	182	2	{0.79}
n2196-56a	56	core	822	14	0.0468	0.0017	7.84	0.27	7.83	0.27	1299	252	2	{0.65}
n2196-82a	82	core	773	18	0.0463	0.0036	8.34	0.39	8.34	0.40	477	130	1	{0.0}
n2196-64a	64	inher. core	4.9	0.1	0.1127	0.0016	1198	66	-	-	286	65	70	0.03
DG23 (Elba, Porto-Azzurro granite)														
n2202-21a	21	core	977	26	0.0450	0.0034	6.59	0.36	6.60	0.36	482	162	1	{1.21}
n2202-23a	23	core	966	18	0.0458	0.0026	6.67	0.25	6.67	0.26	808	385	1	{3.33}
n2202-47a	47	core	1008	17	0.0514	0.0027	6.39	0.22	6.35	0.22	900	404	1	{0.72}
n2202-7a	7	xenocryst	12.4	0.1	0.061	0.001	499	9	-		219	135	23	0.14
DG264 (Giglio monzogranite)														
n2198-3b	3	core	1255	43	0.0455	0.0048	5.14	0.35	5.14	0.36	289	141	-	{3.48}
n2198-3c	3	core	1163	45	0.0491	0.0058	5.54	0.43	5.52	0.44	312	132	-	{4.94}
n2198-5a	5	rim	1136	19	0.0694	0.0067	5.52	0.20	5.50	0.21	2639	591	3	2.58
n2198-8b	8	core	1170	33	0.0529	0.0039	5.51	0.31	5.46	0.31	641	387	1	{2.35}
n2198-8a	8	rim	1174	34	0.0458	0.0038	5.49	0.32	5.49	0.33	604	128	1	{5.07}
n2198-7b	7	inher. core	1.8	0.0	0.236	0.001	2852	60	-		281	373	248	0.02
DG05-1 (Capraia dacite)														
n2707-1b	1	oz rim	874	9	0.0483	0.0024	7.22	0.16	7.35	0.16	1101	682	1	2.0
n2707-1a	1	oz rim	856	8	0.0470	0.0016	7.34	0.14	7.51	0.14	2449	1082	3	2.4
n2707-2a	2	oz rim	868	8	0.0470	0.0017	7.36	0.14	7.42	0.14	2012	1020	3	0.9
n2707-3b	3	core	897	8	0.0514	0.0024	6.98	0.14	7.13	0.14	1266	691	2	2.8
n2707-3a	3	rim	903	11	0.0501	0.0026	6.98	0.18	7.10	0.17	965	335	1	2.2
n2707-4c	4	core	857	12	0.0474	0.0026	7.25	0.23	7.50	0.22	1040	721	-	3.6
n2707-4b	4	oz interm	872	13	0.0464	0.0034	7.14	0.26	7.39	0.24	504	262	-	3.3
n2707-4a	4	oz rim	845	11	0.0394	0.0028	7.29	0.23	7.69	0.20	712	356	-	4.3
n2707-5a	5	oz rim	881	9	0.0500	0.0022	7.21	0.16	7.28	0.16	1413	649	2	1.4
n2707-6a	6	oz rim	834	10	0.0467	0.0026	7.60	0.19	7.72	0.19	851	473	1	1.6
n2707-7a	7	oz rim	850	8	0.0488	0.0017	7.58	0.14	7.55	0.14	2243	1163	3	{0.42}
n2707-8a	8	oz rim	850	8	0.0504	0.0019	7.50	0.14	7.54	0.15	2230	999	3	1.0
n2707-9a	9	oz rim	853	8	0.0509	0.0026	7.39	0.14	7.51	0.15	1597	649	2	2.2
n2707-10a	10	oz rim	853	9	0.0435	0.0026	7.27	0.17	7.58	0.16	863	535	-	3.7
n2707-11a	11	oz rim	848	13	0.0500	0.0030	7.31	0.25	7.56	0.23	686	370	-	3.8
n2707-12a	12	oz rim	863	10	0.0461	0.0020	7.34	0.18	7.47	0.17	1633	540	2	1.7
n2707-12b	12	oz rim	851	11	0.0434	0.0021	7.35	0.21	7.60	0.20	1372	586	-	3.0
n2707-13a	13	oz rim	873	9	0.0507	0.0024	7.21	0.17	7.34	0.16	1268	676	2	2.4

f_{206}% is the percentage of common ^{206}Pb, estimated from the measured ^{204}Pb.
Figures are given in parentheses when no correction has been applied owing to insignificant levels of ^{204}Pb.